NUMERICAL SIMULATION OF THE FLOW OF A POWER LAW FLUID IN AN

ELBOW BEND

A Thesis

by

KARTHIK KANAKAMEDALA

Submitted to the Office of Graduate Studies of
Texas A&M University
in partial fulfillment of the requirements for the degree of

MASTER OF SCIENCE

December 2009

Major Subject: Mechanical Engineering

NUMERICAL SIMULATION OF THE FLOW OF A POWER LAW FLUID IN AN

ELBOW BEND

A Thesis

by

KARTHIK KANAKAMEDALA

Submitted to the Office of Graduate Studies of
Texas A&M University
in partial fulfillment of the requirements for the degree of

MASTER OF SCIENCE

Approved by:

Chair of Committee,	K. R. Rajagopal
Committee Members,	N. K. Anand
	Hamn-Ching Chen
Head of Department,	Dennis O'Neal

December 2009

Major Subject: Mechanical Engineering

ABSTRACT

Numerical Simulation of the Flow of a Power Law Fluid in an Elbow Bend.

(December 2009)

Karthik Kanakamedala, B. Tech, National Institute of Technology Karnataka

Chair of Advisory Committee: Dr. K. R. Rajagopal

A numerical study of flow of power law fluid in an elbow bend has been carried out. The motivation behind this study is to analyze the velocity profiles, especially the pattern of the secondary flow of power law fluid in a bend as there are several important technological applications to which such a problem has relevance. This problem especially finds applications in the polymer processing industries and food industries where the fluid needs to be pumped through bent pipes. Hence, it is very important to study the secondary flow to determine the amount of power required to pump the fluid. This problem also finds application in heat exchangers.

The elbow geometry has been modeled using the software GAMBIT and then the geometry has been imported into FLUENT to carry out the numerical analysis. The problem has been dealt with for both shear thickening and shear thinning fluids. The results have been discussed for different values of power law index, n=0.6, 0.75, 0.9, 1.0, 1.35, 1.45, 1.55 and Re=200, 1100 and aspect ratio, N=0.7, 1.0, 5.0. A total of 42 cases have been simulated.

DEDICATION

I would like to dedicate my thesis to my loving parents and sister.

ACKNOWLEDGEMENTS

NOMENCLATURE

V	Velocity vector
p	Hydrodynamic pressure
T	Cauchy stress tensor
I	Identity tensor
D	Symmetric part of velocity gradient
L	Velocity gradient
μ	Dynamic viscosity of the fluid
μ_e	Effective viscosity
ρ	Density
n	Power law index
Re	Reynolds number
Div	Divergence
Grad	Gradient
N	Aspect ratio of the elbow
L	Length of the straight portion
r	Radius of the elbow bend
R	Radius of the pipe of the elbow

TABLE OF CONTENTS

LIST OF FIGURES

1. INTRODUCTION

This thesis presents the results of the numerical simulation of the governing equations of a power law fluid flowing in an elbow bend. The motivation for the present study is introduced in this chapter. A brief introduction has been given to the non-Newtonian fluid behavior and some of the important literature pertinent to flow through an elbow has been summarized. General remarks about the characteristics of flow through curved pipe are also presented. The introduction will conclude with the objectives and the scope of this study.

1.1 Motivation

When fluid passes through a pipe elbow, the interaction between centrifugal and viscous forces creates a strong secondary flow normal to the pipe axis. This secondary flow consists of two counter-rotating vortices one in either half of the pipe cross section. Since curved sections arise in all piping systems it is important to know the pressure drop in the developing and fully developed parts of the flow if one is to find the pumping power needed to overcome the curvature induced losses due to dissipation. In case of an elbow it would be tough to predict the pressure loss since there are at least two losses superposed- loss due to skin friction and loss due to change in the direction. In addition the secondary flows are expected to enhance heat exchange between the fluid and its surroundings, which is an important factor in designing heat exchangers. So, all these

_____
This thesis follows the style of *IEEE Transactions on Automatic Control*.

issues make the problem of flow through an elbow an interesting one to deal with. The problem of flow of a non-Newtonian fluid through an elbow finds applications in industries such as food industry, polymer processing industry, petroleum industry etc. Therefore the underlying motivation of the present work is to better understand the flow behavior of non-Newtonian fluid through an elbow.

1.2 Fluid Rheology

The Navier-Stokes equations are good for predicting the flow of a wide range of fluids. The constitutive model behind these equations is the linear Newtonian model relating the shear stress and the shear rate governed by the fluid's viscosity which is a constant. Exact solutions to the classical Navier-Stokes equation are very few in number mainly due to the non-linear inertial term in these equations. However, in many of flow problems these terms either disappear automatically due to the constraints involved or are neglected due to their small magnitude resulting in the equations which are linear and can be easily solved. In addition to the Newtonian fluid there is other class of fluids which have complex microstructure such as biological fluids, polymeric liquids, suspensions, liquid crystals whose behavior cannot be explained by the classical linear Newtonian model. Hence, the shear stress cannot be expressed as a linear function of the shear rate. Due to this for such fluids the non-linearities not only occur in the inertial terms but also occur in the viscosity part of the governing equations. Due to these non-linearities it would be very difficult to find the exact solutions for this class of fluids. A better approach to deal with such kind of problems would be the numerical approach.

Now we will go into the details of different kinds of fluids and classify them based on their properties as given by Skelland [1].

1.2.1 Newtonian Fluid

Water at slow speeds can be modeled as a Newtonian fluid. The total stress tensor for a Newtonian fluid can be defined by,

$$\boldsymbol{T} = -p\boldsymbol{I} + 2\mu\boldsymbol{D}$$

where,

$\boldsymbol{T}$ is the total stress tensor

p is the hydrostatic pressure

$\boldsymbol{I}$ is the identity tensor

μ is the dynamic viscosity of the fluid

$\boldsymbol{D}$ is the symmetric part of the velocity gradient

1.2.2 Non-Newtonian Fluid

All those fluids for which the graph plotted between the shear stress and the shear rate is not linear through the origin at a given temperature and pressure can be classified as non-Newtonian fluids. The figure on page 9 shows the rheological behavior of several types fluids. These non-Newtonian fluids can be classified into three categories:

- Time-independent fluids are those for which the rate of shear depends only on the value of the instantaneous shear stress.

- Time-dependent fluids are those for which rate of shear depends on both the magnitude and the duration of shear.

- Viscoelastic fluids are those fluids that exhibit both viscous and elastic properties. They show a partial recovery upon the removal of shear stress.

1.2.2.1 Time-independent Fluids

These fluids are also called "purely viscous fluids" or "non-Newtonian viscous fluids". The shear rate for these fluids does not depend on the duration of shear but only depends on the magnitude of the shear stress applied. These fluids can be further classified into:

- Fluids without yield stress

- Fluids with yield stress (viscoplastic fluids)

The fluids without the yield stress can be further sub divided into:

- Shear thinning fluids

- Shear thickening fluids

1.2.2.2 Shear Thinning Fluids

As the name indicates, the viscosity of these fluids decrease with an increase in the shear rate. The graph plotted between the shear stress and the shear rate is characterized by linearity at very low and very high viscosity. The slopes corresponding to these regions are termed as "zero shear viscosity", $\mu_\circ$ and "infinite shear viscosity",

μ_∞ respectively. Some of the empirical models which have been proposed for relating shear stress and shear rate in pseudoplastic fluids have been discussed below.

1.2.2.3 Power Law Model

The most widely used form of the general constitutive equation is the power law model. The one dimensional power law model during simple shear is given by,

$$\tau_{xy} = K * \left(\dot{\gamma}_{xy}\right)^n$$

where,

τ_{xy} is the shear stress,

K is the consistency index

$\dot{\gamma}_{xy}$ is the rate of shear

n is the power law index

Hence the effective viscosity for a power law model is given by,

$$\mu_{eff} = K * \left(\dot{\gamma}_{xy}\right)^{(n-1)}$$

This is also known as the Ostwald-de Waele power law model and it has gained importance because of its simplicity. But, the main problem with the power law model is that it does not correctly predict the values of zero and infinite values of viscosity. Based on the value of the power law index, 'n' the fluids can be classified into, Shear-thinning fluids for which n is less than 1, Newtonian fluids for which n is 1, Shear-thickening fluids for which n is greater than 1.

1.2.2.4 Cross Model

In order to obtain the required Newtonian region at low and high rates, Cross proposed the model,

$$\frac{\eta - \eta_\infty}{\eta_o - \eta_\infty} = \frac{1}{1 + (K\dot\gamma)^{(1-n)}}$$

where, η_o and η_∞ are zero and infinite shear viscosities respectively and K is the consistency index and $\dot\gamma$ is the rate of shear. These parameters for the model are calculated using the curve fit. It can be seen from the model that for low values of $\dot\gamma$ the value of η goes to η_o and for intermediate values of $\dot\gamma$ the Cross model reduces to a power law region,

$$(\eta - \eta_\infty) = (\eta_o - \eta_\infty)m\dot\gamma^{(n-1)}$$

where, $m = K^{(n-1)}$ and for $\eta \gg \eta_\infty$

$$\eta \cong \eta_o m\dot\gamma^{(n-1)}$$

1.2.2.5 Carreau Model

A model that more clearly captures more details of the experimentally measured $\eta(\dot\gamma)$ is the Carreau-Yasuda model. It uses five parameter model compared to the two parameters of the power law model. The Carreau-Yasuda model is given below.

$$\frac{\eta(\dot\gamma) - \eta_\infty}{\eta_o - \eta_\infty} = [1 + (\lambda\dot\gamma)^a]^{\frac{n-1}{a}}$$

where, η_o and η_∞ are zero and infinite viscosities respectively. λ is the time constant for the fluid which determines the shear rate at which the transition takes place from the zero-shear rate plateau to the power law portion and also the transition from power law

region to $\eta = \eta_\infty$ and n is power law index which depends on the slope of the rapidly decreasing portion of the curve.

In the model developed by Bird and Carreau the value 'a' was assumed to be 2 and hence, reducing the number of parameters to be fit to four. The Bird Carreau model was given as,

$$\frac{\eta(\dot{\gamma}) - \eta_\infty}{\eta_o - \eta_\infty} = [1 + (\lambda\dot{\gamma})^2]^{\frac{n-1}{2}}$$

1.2.2.6 Ellis Model

In the model proposed by Ellis, the apparent viscosity varies as function given by,

$$\frac{\eta_o}{\eta} = 1 + \left(\frac{\tau_{12}}{\tau_{1/2}}\right)^{(\beta-1)}$$

where, η_o is the zero viscosity, β is a dimensionless parameter. τ_{12} is the shear stress and $\tau_{1/2}$ is the shear stress at $\eta = \eta_o/2$. The Ellis model is a three parameter model and has advantage of having a limiting viscosity, η_o at zero shear rate and shear thinning viscosity at higher shear rate. The exponent in the gives describes the rate at which the curve between viscosity and shear rate falls down and describes the shear thinning behavior.

1.2.2.7 Dilatant Fluids

Two phenomena have been observed with dilatants fluids. Volumetric dilatancy denotes an increase in total volume under shear, whereas as rheological dilatancy implies an increase in the apparent viscosity with increasing shear rate. The later is the most common among the dilatants fluids. These dilatants fluids are far less common than the pseudoplastic fluids. Some of the models which can be used for modeling such kind of fluids have already been discussed above.

The reason behind such kind of behavior can be explained as follows. In case of suspensions the particles will be oriented at rest so that the void space is the minimum. The liquid in the suspension in this case is just sufficient to fill the voids. But when the suspension is sheared the space between particles becomes incompletely filled with liquid. Under these conditions of inadequate lubrication the surfaces of adjacent particles come in contact with each other resulting in the increase of friction and hence the shear stress increases with increase in shear rate.
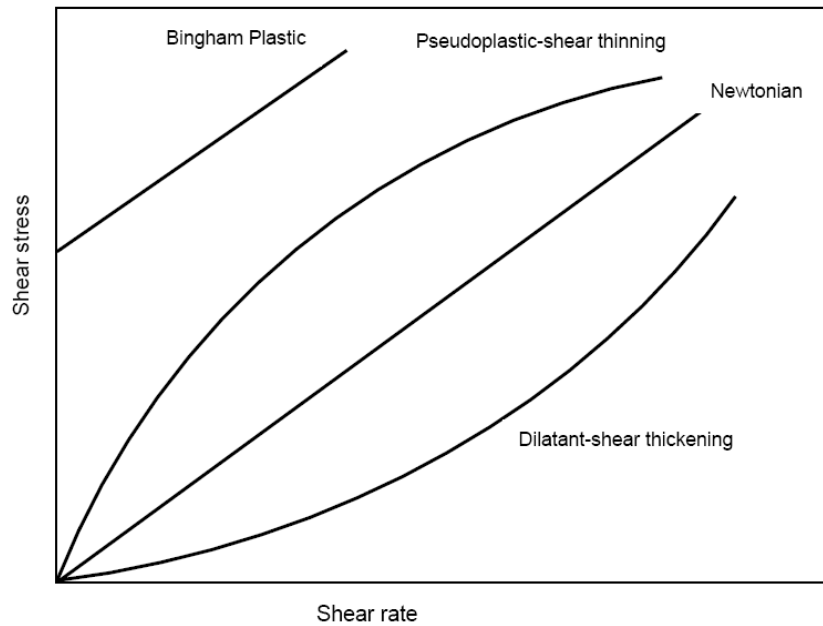
Figure 1.1. Graph of shear stress vs. shear strain for Newtonian and non-Newtonian

fluids

In a simple shear flow, the relationship between shear stress and shear strain for Newtonian and non- Newtonian fluids is given by relationship as depicted in figure 1.1.

1.2.2.8 Time Dependent Fluids

The time dependent fluids can be classified into two groups based on the variation of the shear stress with time at a given shear rate and constant temperature.

- Thixotropic fluids
- Rheopectic fluids

1.2.2.9 Thixotropic Fluids

These fluids exhibit a reversible decrease in shear stress with time at a constant rate of shear and fixed temperature. If the flow curve is measured in a single experiment in which the shear rate is steadily increased from zero to a maximum value and then decreased to zero then a hysteresis loop will be obtained. Thus altering the rate at which the shear rate is increased or decreased alters the shape of the hysteresis loop. Some of the examples of thixotropic materials are melts of high polymers, paints, greases, printing inks.

1.2.2.10 Rheopectic Fluids

These materials also referred to as antithixotropic fluids, are relatively rare in occurrence. They exhibit a reversible increase in shear stress with time at a constant rate of shear under isothermal conditions. Hence, the hysteresis loop obtained for these materials is exactly opposite to that obtained for thixotropic materials. Some examples of these kinds of materials are bentonite clay suspensions, gypsum suspensions.

1.2.2.11 Viscoelastic Fluids

These materials exhibit both viscous and elastic properties. In a purely Hookean elastic solid the stress corresponding to given strain is independent of time whereas in case of viscoelastic materials the stress relaxes gradually. In contrast to purely viscous liquid, the viscoelastic fluids flow when subjected to stress a part of their deformation is

recovered upon the removal of the stress. Some of the examples of viscoelastic fluids are bitumens, flour dough, polymer and polymer melts such as nylon.

1.3 Literature Review

In this section we will briefly look into some of important research work that has been done related to the problem of power law fluid in a bend. Bandhyopadhyay and Das [2] did experimental investigations to determine the pressure drop across different piping components like orifices, gate and globe valves, elbows and bends for pseudoplastic liquid in laminar flows. Empirical correlations have been developed for the friction factor in an elbow using different non dimensional parameters. Marn and Ternik[3] studied the flow of shear thickening fluid numerically to obtain the pressure loss coefficient. A quadratic model has been used to model the shear thickening mixture of electrostatic ash and water mixture. The results have been obtained for small curvature radius. A CFX code has been written to solve the problem and the code employs finite element method. Bandhyopadhyay, Benerjee and Das [4] carried out experimental investigations to determine the pressure loss of a gas non-Newtonian liquid flow through an elbow in the horizontal plane. An empirical relation has been developed to find the pressure drop as a function of various variables of the problem. A power law model has been used to model the shear thinning non-Newtonian fluids and liquid used for experiments was salt of Carboxy Methyl Cellulose (SCMC). A comprehensive review on the flow in curved tubes has been done by Berger, Talbot and Yao [5]. They have also discussed the various details of secondary flows. Few researchers like Arada et

al. [6] used finite element methods to obtain the solution for steady fully developed generalized Newtonian flows in a curved pipe of circular cross-section. It was concluded that small changes on the viscosity parameters influence the distribution of axial velocity and wall shear stress for small and intermediate curvature ratio. Soh and Berger [7] performed the analysis for large values of curvature ratio. ADI finite difference scheme has been used to numerically solve the Navier-Stokes equations. All the computations were performed on a Newtonian fluid. It was concluded that the assumption of very small curvature ratio is reasonable and produces results with an error of 10%, but full Navier stokes equation need to be solved for finding the exact solution. A new finite difference scheme has been discussed by Dennis [8] to solve the governing equations of steady state viscous fluid through a curved tube of circular cross-section. The Navier stokes have been solved using a finite difference scheme of second order accuracy. Raju and Rathna [9] extended the work done by Rathna [10]. They studied the problem of heat transfer of power law fluid flowing through a curved pipe. The problem has been solved by assuming the curvature ratio to be small. It was found that the fluid is heated throughout for lower prandtl number but for higher prandtl number it creates heated and cooled regions. It was also concluded that dilatants fluids are better for heat exchangers. Hsu and Patankar [11] solved the laminar fully developed flow in a curved tube numerically for a Power law fluid. Results for the velocity and temperature field, friction factor and Nusselt numbers were obtained for different prandtl number and power law index. Shobha et al. [12] studied fully developed isothermal, incompressible laminar flow of power law fluids small tube radius to the radius of curvature. The effect of the

Reynolds number, curvature ratio and power law index was discussed. Solutions

obtained for both primary and secondary flow have been analyzed. Takami, Sudou and

Tomita [13] have studied fully developed laminar flow of power law fluids through

curved tubes for different curvature ratios and power law index. The problem has been

solved for shear thinning fluids. The effect of Reynolds number on the flow has also

been considered. Another important work has been done by Homicz [14] in which he

investigated the flow accelerated corrosion in a pipe elbow. The flow condition

considered was turbulent and the computational fluid dynamic simulations have been

carried out using FLUENT.

1.4 Objectives of the Present Study

The main objectives of the present study are:

1. To find the effect of various parameters such as Reynolds number, aspect ratio and power law index on the velocity contours in the elbow.

2. To determine the importance and the magnitude of the secondary flow in each case simulated.

3. Find the magnitude of shear stress in different parts of the elbow.

2. PRELIMINARIES

In this section some of the basic concepts of continuum mechanics have been summarized. First we go through some basic definitions in kinematics. Then the basic balance laws namely balance of mass, balance of linear and angular momentum and balance of energy have been discussed.

2.1 Kinematics

Kinematics deals with the motion and the deformation of material bodies without resorting to any description of the outside influence which causes it.

Let B be any abstract body. Let $K_R(B)$ denote the reference configuration of the body B and $K_t(B)$ denote the current configuration at time, t. Now we can associate a one to one mapping χ (assumed to be sufficiently smooth), which represents the motion of the body (as shown in figure 2.1) and that assigns to each point $\boldsymbol{X}$ belonging to K_R, a point $\boldsymbol{x}$ belonging to K_t, for each time t, i.e.

$$\boldsymbol{x} = \chi(\boldsymbol{X}, t) \ \text{ or } \ \boldsymbol{X} = \chi^{-1}(\boldsymbol{x}, t)$$
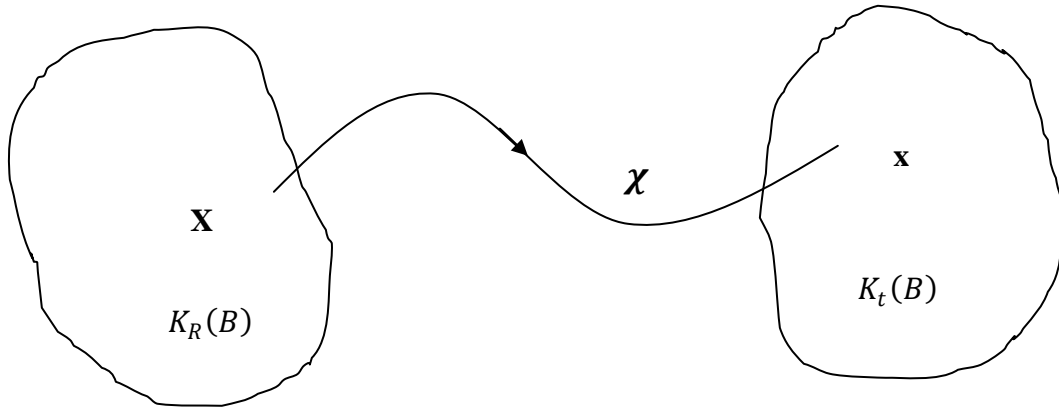
Figure 2.1. Motion of the body

Any property of the body, ϕ can be expressed either as a function of (X, t) or as a function of (x, t). So we can either talk about the property of a particle which is in $K_R(B)$ was at X at time t or the property of a particle which in $K_t(B)$ is at x at time t, i.e.,

$$\phi = \hat{\phi}(X, t) = \tilde{\phi}(x, t)$$

$\phi = \hat{\phi}(X, t)$ is a Lagrangian specification since the observation is made with respect to the reference configuration. Now, if the observation is made with respect to the current configuration then it is called the Eulerian motion i.e $\phi = \tilde{\phi}(x, t)$ is an Eulerian specification.

The velocity of the particle is given by,

$$v(X, t) = \frac{\partial \chi}{\partial t}$$

And, the acceleration is

$$a(X,t) = \frac{\partial^2 \chi}{\partial t^2}$$

Using the definition of the motion, χ we can now define the deformation gradient

of the motion, F as,

$$F = \frac{\partial x}{\partial X}$$

Now, using the definition of F, we can define the left and right Cauchy-Green

stretch tensors, B and C to be,

$$B = FF^T \quad , \qquad C = F^T F$$

The velocity gradient L is defined as,

$$L = grad(V) = \frac{\partial V}{\partial X}$$

using the definition of F and L it can be reduced that,

$$L = \dot{F}F^{-1}$$

The symmetric part of L (often referred to as the rate of deformation tensor) is given by,

$$D = \frac{1}{2}(L + L^T)$$

and, the skew part (often referred to as the spin tensor) is given by,

$$W = \frac{1}{2}(L - L^T)$$

2.2 Balance of Mass

2.2.1 Lagrangian Form

Let $K_R(B)$ and $K_t(B)$ represent reference and current configurations of an abstract body, B.

Let, $P_t(B) = K_t\big(P_R(B)\big)$ $\qquad\qquad \forall\, P_R(B) \subseteq K_R(B)$

From the statement of balance of mass we get,

$$\int_{P_R} \rho_R\, dV = \int_{P_t} \rho_t\, dv \qquad\qquad \forall\, P_R(B) \subseteq K_R(B)$$

Now, let the density at time t, ρ_t be denoted by ρ, and ρ_R denotes the density in the reference configuration.

Thus,

$$\int_{P_R} \rho_R\, dV = \int_{P_t} \rho\, dv = \int_{P_R} \rho\, \det(F)\, dV \qquad\qquad \forall\, P_R(B) \subseteq K_R(B)$$

$$\Rightarrow \int_{P_R} \int \big(\rho_R - \rho\, \det(F)\big)\, dV = 0 \qquad\qquad \forall\, P_R(B) \subseteq K_R(B)$$

Thus, if the integrand is continuous we can conclude that,

$$\rho_R = \rho\, \det(F)$$

This is known as the Langrangian form of balance of mass.

2.2.2 Eulerian Form

Let P_t be a sub-body ($\subseteq K_t(B)$). Then balance of mass can be expressed as,

$$\frac{d}{dt} \int_{P_t} \rho\, dV = 0 \qquad\qquad \forall\, P_t(B) \subseteq K_t(B)$$

Above equation can be reduced to,

$$\int_{P_t} [\frac{d\rho}{dt} + \rho \; div(\boldsymbol{v})] \; dv = 0 \qquad\qquad \forall \; P_t(B) \subseteq K_t(B)$$

If the integrand is continuous,

$$\frac{d\rho}{dt} + \rho \; div(\boldsymbol{v}) = 0$$

Hence, we obtain

$$\frac{\partial\rho}{\partial t} + div(\rho\boldsymbol{v}) = 0$$

This is the Eulerian form of balance of mass. If the material is incompressible then we obtain,

$$div(\boldsymbol{v}) = 0 \qquad or \qquad \det(\boldsymbol{F}) = 1$$

2.3 Balance of Linear Momentum

The balance of linear momentum is the application of Newton's law of motion to a continuum. The Eulerian form of the balance of linear momentum is given by,

$$div(\boldsymbol{T}^T) + \rho\boldsymbol{b} = \rho\frac{D\boldsymbol{v}}{Dt}$$

$$\Rightarrow div(\boldsymbol{T}^T) + \rho\boldsymbol{b} = \rho(\frac{\partial\boldsymbol{v}}{\partial t} + (\nabla\boldsymbol{v})\boldsymbol{v})$$

where, $\boldsymbol{T}$ is the Cauchy stress tensor, $\boldsymbol{b}$ is the body force, $\boldsymbol{v}$ is the velocity vector and ρ is the density of the body.

In the absence of internal couples, the conservation of angular momentum reduces to

$$T = T^T$$

i.e., Cauchy stress tensor is symmetric.

2.4 Balance of Energy

 According to the balance of energy, the change in energy of the system is equal to the transfer of energy to the system. For a thermomechanical process, the balance of energy is given as,

$$\rho\epsilon + div(q) = T.L + \rho r$$

where,

ϵ is the internal energy

q is the heat flux

r is the heat radiated

2.5 Governing Equations

 The constitutive model relating the Cauchy shear stress and the velocity gradients for a linearly viscous incompressible fluid (Newtonian fluid) is given by,

$$T = -pI + 2\mu D$$

where,

T is the Cauchy shear stress

p is the hydrodynamic pressure

I is the Identity tensor

μ is the viscosity of the fluid

$\boldsymbol{D}$ is the symmetric part of velocity gradient

Since, an incompressible fluid undergoes an isochoric motion,

$$\det(\boldsymbol{F}) = 1$$

From this it can also be obtained that for an incompressible fluid,

$$div(\boldsymbol{v}) = 0$$

By substituting for the constitutive equation in the balance of linear momentum we obtain the Navier Stokes equation for a Newtonian fluid. The Navier Stokes equations are given by,

$$\rho \frac{D\boldsymbol{v}}{Dt} = -\frac{\partial p}{\partial \boldsymbol{x}} + \rho\boldsymbol{b} + \mu\Delta\boldsymbol{v}$$

where,

Δ is the Laplacian operator

ρ is the density of the body

$\boldsymbol{b}$ is the body force

$\boldsymbol{v}$ is the velocity vector

However, the fluid being dealt within the problem is a non-Newtonian power law fluid and the model is given by Malek, Rajagopal and Ruzicka [15],

$$\boldsymbol{T} = -p\boldsymbol{I} + \mu_0[1 + \alpha(tr\,\boldsymbol{D}^2)]^{\frac{n-1}{2}}\boldsymbol{D}$$

where,

μ_0 and α are model parameters

n is power law index

If the power law index, n is less than one then the fluid is a shear thinning fluid, which means the viscosity decreases with an increase in rate of shear. But, if n takes the value 1, then the model represents a Newtonian fluid for which the viscosity is a constant. If n is greater than 1 then the fluid is a shear thickening fluid i.e., viscosity increases with an increase in the rate of shear.

The term $\mu_o[1 + \alpha(tr\,\mathbf{D}^2)]^{\frac{n-1}{2}}$ is called the generalized viscosity term for the fluid and is representing in the following sections by μ_e.

Using the model for the stress tensor the governing equations for the fluid have been derived by substituting for the stress tensor in the balance of linear momentum. The final form of the simplified momentum equations is given by,

R-momentum,

$$\rho\left[\frac{\partial u_r}{\partial t} + u_r\frac{\partial u_r}{\partial r} + \frac{u_\theta}{r}\frac{\partial u_r}{\partial \theta} + u_x\frac{\partial u_r}{\partial x} - \frac{u_\theta}{r}\right]$$

$$= -\frac{\partial p}{\partial r} + \mu_0 n\alpha(C_1)^{\frac{(n-1)}{2}-1}\left[\frac{C_3}{2r}\left(r\frac{\partial}{\partial r}\left(\frac{u_\theta}{r}\right) + \frac{1}{r}\frac{\partial u_r}{\partial \theta}\right)\right]$$

$$+\mu_0 n\alpha(C_1)^{\frac{(n-1)}{2}-1}\left[C_2\left(\frac{\partial u_r}{\partial r}\right) + \frac{C_4}{2}\left(\frac{\partial u_r}{\partial x} + \frac{\partial u_x}{\partial r}\right)\right] + \mu_e\left[\frac{1}{2}\Delta u_r - \frac{u_r}{2r^2} - \frac{1}{r^2}\frac{\partial u_r}{\partial \theta}\right]$$

θ-momentum,

$$\rho\left[\frac{\partial u_\theta}{\partial t} + u_r\frac{\partial u_\theta}{\partial r} + \frac{u_\theta}{r}\frac{\partial u_\theta}{\partial \theta} + u_x\frac{\partial u_\theta}{\partial x} + \frac{u_r u_\theta}{r}\right]$$

$$= -\frac{1}{r}\frac{\partial p}{\partial \theta} + \mu_0 n\alpha(C_1)^{\frac{(n-1)}{2}-1}\left[\frac{C_3}{r}\left(\frac{1}{r}\frac{\partial u_\theta}{\partial \theta} + \frac{u_r}{r}\right)\right]$$

$$+\mu_0 n\alpha(C_1)^{\frac{(n-1)}{2}-1}\left[\frac{C_2}{2}\left(r\frac{\partial}{\partial\theta}\left(\frac{u_\theta}{r}\right)+\frac{1}{r}\frac{\partial u_r}{\partial\theta}\right)\right]+\mu_0 n\alpha(C_1)^{\frac{(n-1)}{2}-1}\left[\frac{C_4}{2}\left(\frac{\partial u_\theta}{\partial x}+\frac{1}{r}\frac{\partial u_x}{\partial\theta}\right)\right]$$

$$+\mu_e\left[\frac{1}{2}\Delta u_\theta-\frac{u_\theta}{2r^2}+\frac{1}{r^2}\frac{\partial u_r}{\partial\theta}\right]$$

X-momentum,

$$\rho\left[\frac{\partial u_\theta}{\partial t}+u_r\frac{\partial u_\theta}{\partial r}+\frac{u_\theta}{r}\frac{\partial u_x}{\partial\theta}+u_x\frac{\partial u_x}{\partial x}\right]$$

$$=-\frac{\partial p}{\partial x}+\mu_0 n\alpha(C_1)^{\frac{(n-1)}{2}-1}\left[\frac{C_2}{2}\left(\frac{\partial u_r}{\partial x}+\frac{\partial u_x}{\partial r}\right)\right]$$

$$+\mu_0 n\alpha(C_1)^{\frac{(n-1)}{2}-1}\left[\frac{C_3}{2r}\left(\frac{\partial u_\theta}{\partial x}+\frac{1}{r}\frac{\partial u_x}{\partial\theta}\right)+C_4\left(\frac{\partial u_x}{\partial x}\right)\right]+\frac{\mu_e}{2}\left(\Delta u_x\right)$$

where, C_1, C_2, C_3, C_4 are given by,

$$C_1=1+\alpha(tr\,\mathbf{D}^2)$$

$$=1+\alpha\left[\left(\frac{\partial u_r}{\partial r}\right)^2+\left(\frac{1}{r}\frac{\partial u_\theta}{\partial\theta}+\frac{u_r}{r}\right)^2+\left(\frac{\partial u_x}{\partial x}\right)^2+\frac{1}{2}\left(r\frac{\partial}{\partial r}\left(\frac{u_\theta}{r}\right)+\frac{1}{r}\frac{\partial u_r}{\partial\theta}\right)^2\right.$$

$$\left.+\frac{1}{2}\left(\frac{\partial u_r}{\partial x}+\frac{\partial u_x}{\partial r}\right)^2\right]$$

$$+\alpha\left[\frac{1}{2}\left(\frac{\partial u_\theta}{\partial x}+\frac{1}{r}\frac{\partial u_x}{\partial\theta}\right)^2\right]$$

$$C_2=\frac{\partial}{\partial x}(tr\,\mathbf{D}^2)$$

$$=2\left(\frac{\partial u_r}{\partial r}\right)\left(\frac{\partial^2 u_r}{\partial r^2}\right)+2\left(\frac{1}{r}\frac{\partial u_\theta}{\partial\theta}+\frac{u_r}{r}\right)\times\frac{\partial}{\partial r}\left(\frac{1}{r}\frac{\partial u_\theta}{\partial\theta}+\frac{u_r}{r}\right)+2\left(\frac{\partial u_x}{\partial x}\right)\left(\frac{\partial^2 u_x}{\partial x\partial r}\right)$$

$$+\left(r\frac{\partial}{\partial\theta}\left(\frac{u_\theta}{r}\right)+\frac{1}{r}\frac{\partial u_r}{\partial\theta}\right)\times\frac{\partial}{\partial r}\left(r\frac{\partial}{\partial\theta}\left(\frac{u_\theta}{r}\right)+\frac{1}{r}\frac{\partial u_r}{\partial\theta}\right)+\left(\frac{\partial u_r}{\partial x}+\frac{\partial u_x}{\partial r}\right)$$

$$\times\frac{\partial}{\partial r}\left(\frac{\partial u_r}{\partial x}+\frac{\partial u_x}{\partial r}\right)$$

$$+ \left(\frac{\partial u_\theta}{\partial x} + \frac{1}{r}\frac{\partial u_x}{\partial \theta} \right) \times \frac{\partial}{\partial r} \left(\frac{\partial u_\theta}{\partial x} + \frac{1}{r}\frac{\partial u_x}{\partial \theta} \right)$$

$$C_3 = \frac{\partial}{\partial \theta}(tr\ \boldsymbol{D}^2)$$

$$= 2\left(\frac{\partial u_r}{\partial r} \right)\left(\frac{\partial^2 u_r}{\partial r \partial \theta} \right) + 2\left(\frac{1}{r}\frac{\partial u_\theta}{\partial \theta} + \frac{u_r}{r} \right) \times \frac{\partial}{\partial \theta}\left(\frac{1}{r}\frac{\partial u_\theta}{\partial \theta} + \frac{u_r}{r} \right) + 2\left(\frac{\partial u_x}{\partial x} \right)\left(\frac{\partial^2 u_x}{\partial x \partial \theta} \right)$$

$$+ \left(r\frac{\partial}{\partial r}\left(\frac{u_\theta}{r} \right) + \frac{1}{r}\frac{\partial u_r}{\partial \theta} \right) \times \frac{\partial}{\partial \theta}\left(r\frac{\partial}{\partial r}\left(\frac{u_\theta}{r} \right) + \frac{1}{r}\frac{\partial u_r}{\partial \theta} \right) + \left(\frac{\partial u_r}{\partial x} + \frac{\partial u_x}{\partial r} \right)$$

$$\times \frac{\partial}{\partial \theta}\left(\frac{\partial u_r}{\partial x} + \frac{\partial u_x}{\partial r} \right)$$

$$+ \left(\frac{\partial u_\theta}{\partial x} + \frac{1}{r}\frac{\partial u_x}{\partial \theta} \right) \times \frac{\partial}{\partial \theta}\left(\frac{\partial u_\theta}{\partial x} + \frac{1}{r}\frac{\partial u_x}{\partial \theta} \right)$$

$$C_4 = \frac{\partial}{\partial x}(tr\ \boldsymbol{D}^2)$$

$$= 2\left(\frac{\partial u_r}{\partial r} \right)\left(\frac{\partial^2 u_r}{\partial r \partial x} \right) + 2\left(\frac{1}{r}\frac{\partial u_\theta}{\partial \theta} + \frac{u_r}{r} \right) \times \frac{\partial}{\partial x}\left(\frac{1}{r}\frac{\partial u_\theta}{\partial \theta} + \frac{u_r}{r} \right) + 2\left(\frac{\partial u_x}{\partial x} \right)\left(\frac{\partial^2 u_x}{\partial x^2} \right)$$

$$+ \left(r\frac{\partial}{\partial r}\left(\frac{u_\theta}{r} \right) + \frac{1}{r}\frac{\partial u_r}{\partial \theta} \right) \times \frac{\partial}{\partial x}\left(r\frac{\partial}{\partial r}\left(\frac{u_\theta}{r} \right) + \frac{1}{r}\frac{\partial u_r}{\partial \theta} \right) + \left(\frac{\partial u_r}{\partial x} + \frac{\partial u_x}{\partial r} \right)$$

$$\times \frac{\partial}{\partial x}\left(\frac{\partial u_r}{\partial x} + \frac{\partial u_x}{\partial r} \right)$$

$$+ \left(\frac{\partial u_\theta}{\partial x} + \frac{1}{r}\frac{\partial u_x}{\partial \theta} \right) \times \frac{\partial}{\partial x}\left(\frac{\partial u_\theta}{\partial x} + \frac{1}{r}\frac{\partial u_x}{\partial \theta} \right)$$

And the Generalized viscosity function is given by,

$$\mu_e = \mu_0[1 + \alpha(tr\ \boldsymbol{D}^2)]^{\frac{(n-1)}{2}}$$

3. PROBLEM DESCRIPTION AND PROCEDURE

3.1 Problem Description

The problem of flow of power law fluid through an elbow has been simulated. A parametric analysis has been done carried out by varying various geometry and flow parameters. This problem finds applications mainly in the food and polymer industries where non-Newtonian fluids flow through different piping sections.

The elbow geometry used for performing the simulations consists of a straight portion of 'L' both after the inlet and before the exit. Between the two straight portions it consists of a bend of radius 'r'. The diameter of the elbow is kept constant, 'D'. The power law index 'n' of the fluid has also been varied. The simulations have been done for shear thinning, Newtonian as well as shear thickening fluids. The dimensions of the elbow considered in different cases are,

Diameter of the elbow $(D) = 0.02$m

Radius of the elbow $(r) = 0.02$m

Considering the non-dimensional parameter, $N = \frac{L}{r}$, different values of N were considered to obtain the results for both short as well as long elbows. The different values of N chosen are $N= 0.7, 1.0, 5.0$. We refer to N as the aspect ratio in subsequent sections.

Figure 3.1 shows the top view of the elbow geometry used in the fluid simulations. The (x, y) coordinates are in the plane of the paper and z is positive out of the paper.
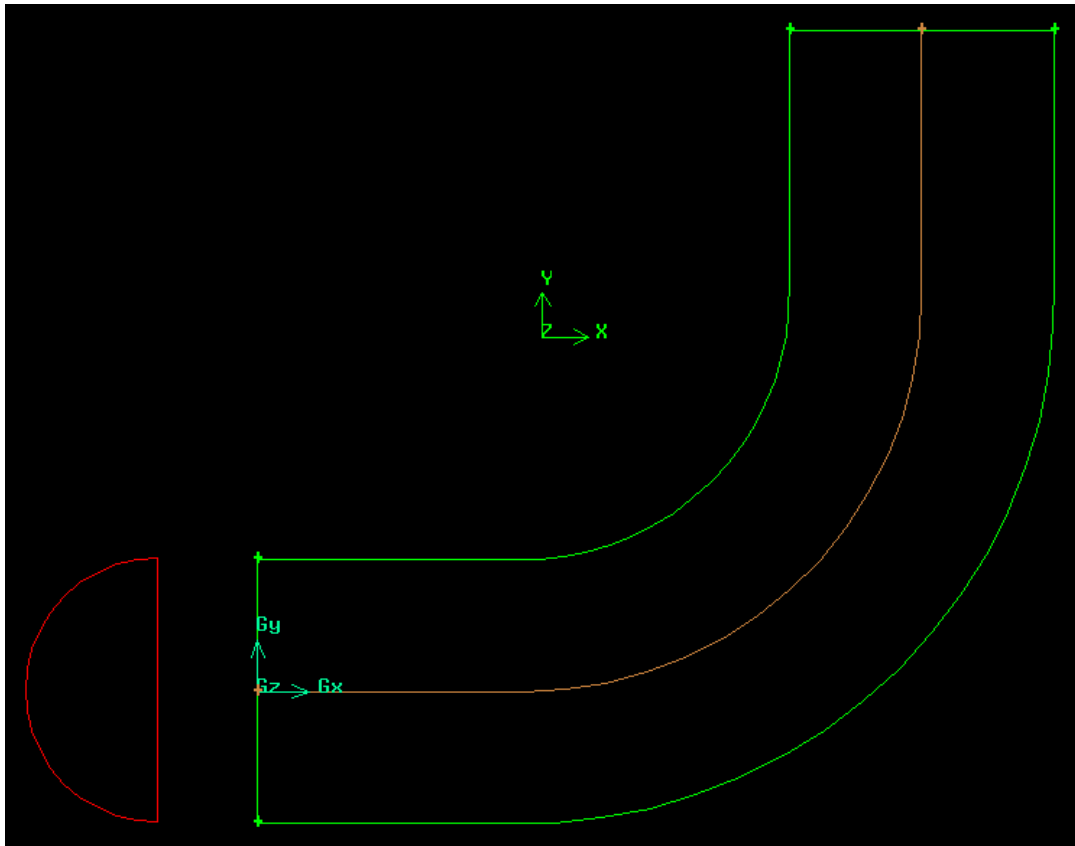
Figure 3.1. Geometry of the problem

Next, besides the geometry parameters flow properties have also been varied. The main flow properties studied are the power law index and Reynolds number.

First, the most important flow property studied is the power law index of the fluid. The simulations have been done for shear thinning, Newtonian as well as shear thickening fluids. The different values of n considered for the simulations are 0.6, 0.75, 0.90, 1.00, 1.35, 1.45, 1.55.

Besides the power law index the other flow property that has been varied is the Reynolds number. The flow is assumed to be laminar and hence two Reynolds numbers have been considered, Re=200, 1100 i.e. one at the higher end and the other at the lower end. The Reynolds number for a power law fluid as given by [16],

$$Re = \left(\frac{4n}{3n+1}\right)^n \frac{\rho D^n V^{2-n}}{\mu_0 8^{n-1}}$$

where,

Re is the Reynolds number

n is the power law index

D is the diameter of the pipe

μ_0 is the dynamic viscosity of the fluid

ρ is the density of the fluid

3.2 Procedure

First the geometry was generated using GAMBIT version 2.3.16. For creating the geometry, first vertices have been created in the plane $Z=0$. For creating the geometry, first the vertices have been created in the plane $Z=0$. After creating the two dimensional geometry a face created at the inlet. The face created at the inlet was swept along the axis of the elbow resulting in a three dimensional geometry.

Next, the geometry needs to be meshed. A structured mesh was used to mesh the geometry. First step in meshing the geometry is to mesh the edges. The edges along the

axis were meshed using bell-shaped elements. The edges both at the inlet and the exit were also meshed.

Next after meshing the edges a boundary layer mesh was created. The mesh is greatly refined in the vicinity of the pipe wall, in order to capture the large gradients in the viscous boundary layer. The cell adjacent to the wall is specified to have a thickness of 0.3mm; the cell thickness gradually increases with the distance from the wall at a ratio of 1.1. This results in a boundary layer of 2.8mm (number of rows is specified to be 7).

The mesh outside the boundary layer was created by paving the remaining area with quadrilateral elements with an interval size of 0.9mm. The 2D surface mesh thus formed was swept along the axis to form volume mesh consisting of hexagonal cells. Hence, the cross-sectional view of the mesh is the same throughout the elbow.
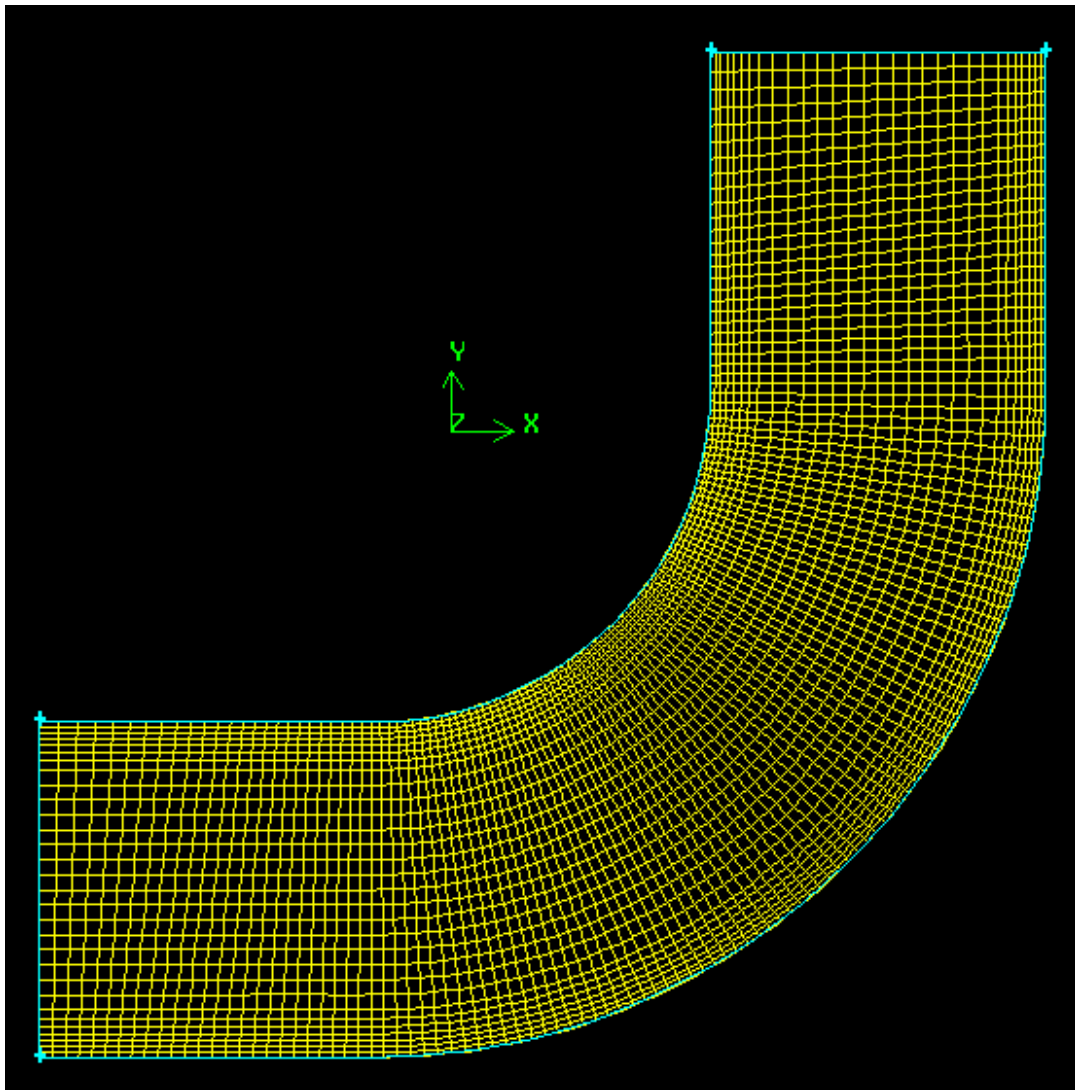
Figure 3.2. Top view of the meshed symmetry face

Figure 3.2 shows the mesh on the symmetry plane of the elbow section. Figure 3.3 shows the cross sectional view of the mesh in the elbow. Again, the boundary layer mesh applied to the wall is clearly visible. The resulting volume mesh consisted of around 49,000 nodes and 45,000 elements.
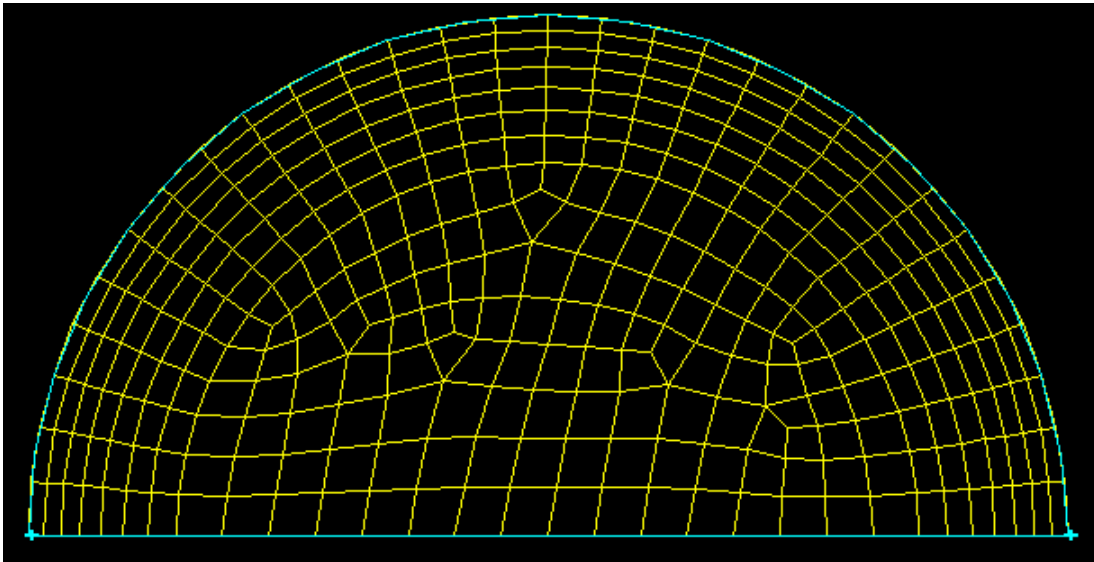
Figure 3.3. Cross-sectional view of the mesh

After creating the mesh, the zones have to be assigned to the model. The zones assigned were wall, velocity inlet, pressure outlet and symmetry to the four faces.

After assigning the zone types the next step is to import the mesh file into FLUENT. The FLUENT version used was 6.3.26. After importing the meshed geometry into FLUENT the grid is first checked for irregularities. The grid check is done to make sure the grid is ready to be for the analysis. After the grid check can be scaled if required.

The mesh is now ready to be used. Next all the variables such as temperature, pressure, velocity, density, length are set to SI units (default settings).

The viscosity function is written using C-Programming and is then imported as an interpreted user-defined function. We need to compile this program and check for any errors in the main window.

Next, the solver is set to a Pressure-based solver and the implicit type of formulation is selected from the menu. Three dimensional space is chosen for the analysis and the velocity formulation is kept as absolute (default settings).

Next, the material needs to be defined. New materials can be created by selecting different properties and entering the values of each specified property. Here, it should be noted that except for viscosity all the remaining properties of the material are chosen to be constant. Hence, for the properties like density, thermal conductivity, specific heat 'constant' is selected from the drop down menu. But for the viscosity, 'user-defined function' is selected from the drop down menu which brings up a pop up of the compiled user defined function from which the program written for the viscosity function needs to be selected. Hence, this program will be used to calculate the changes in the viscosity at every iteration using the values from the previous iteration.

Now, having specified the materials the boundary conditions need to be specified to solve the problem. The surfaces bordering the fluid domain fall into four categories: 1) the symmetry plane 2) the plane surface at $x = 0$ where the fluid enters, referred to as the inlet 3) thirdly, it is the solid pipe which is assigned the wall boundary having a no slip condition the pipe surface 4) lastly, the face at which the fluid exits at the right top corner is referred to as the outlet. All these boundary conditions have been discussed in the subsequent paragraphs.

Since the flow is treated as isothermal and the gravitational effects are neglected the flow can be assumed to be symmetric about the plane $z = 0$. Therefore our model includes the flow only on the side of positive z. This is accomplished in FLUENT by setting a symmetry boundary condition to this plane. Then the FLUENT sets the velocity perpendicular to this boundary as zero i.e. the z-component of the velocity at the boundary is zero. It also sets the gradient of flow variables normal to the boundary as zero. i.e $\partial(\ldots)/\partial n = 0$ at $z = 0$.

Since it is a velocity boundary condition at the inlet, the components of the velocity at the inlet plane are given as the input conditions. The inlet velocity is calculated using the Reynolds number relation which was discussed previously.

For a non-porous wall the component of velocity normal to the wall is zero. In addition to this, since we are treating the flow to be viscous the no-slip boundary condition holds good due to which all the three components of velocity on the wall are zero.

At the outlet face, the FLUENT's pressure outlet boundary condition is applied. This boundary condition requires the input of gauge static pressure. As the outlet was assumed to be at the atmospheric pressure, the gauge pressure would be zero and hence all the default settings in FLUENT have been retained.

Having set up the boundary conditions, the next step is to solve the problem. For this first the solution controls need to be set up. The Navier Stokes equations, which express conservation of mass and momentum, form a coupled set of nonlinear PDE's. FLUENT uses finite volume discretization method in order to convert these into a set of

non-linear algebraic equations. The solutions obtained here employ the segregated solution algorithm, in which the equations are solved sequentially, instead of solving them simultaneously using matrix method. Now, as the equations are non-linear and coupled, an iterative process should be used starting from an initial guess value for all the variables, and the solution is allowed to relax to the final solution as the iterations proceed.

So in order to achieve this in FLUENT first the solution controls need to be set up. FLUENT's "standard" scheme is used for the pressure interpolation while the convective and viscous terms in the momentum equations are discretized using "Power Law" scheme. SIMPLE algorithm has been used to solve the pressure velocity coupled equations. The relaxation factors for the pressure and momentum were chosen to be 0.3, 0.5 respectively.

Having set up all the solution controls the next step is to initialize all the flow variables in order to start the iterations. Constant values have been chosen throughout the mesh for all flow variables: (u, v, w, p) have been set to (0, 0, 0, 0) in all the cells.

As the flow variables have been initialized the next step is to set the convergence criteria of the iteration process. The residuals of the continuity equation, x-velocity, y-velocity and z-velocity have been monitored and solutions have been obtained up to an accuracy of 10^{-5}.

Now the iterations can be carried out by monitoring the solution and the residuals were plotted after every iteration. Simulations were done for three geometries for N=0.7, 1.0, 5.0 with the power law index as n= 0.60, 0.75, 0.90, 1.00, 1.35, 1.45, 1.55. All these

cases have been simulated for two Reynolds numbers, $Re =$200, 1100. So, a total of 42 cases were simulated.

After carrying out the simulations the grid independence of the solution needs to be checked. The mesh has been refined by increasing the number of elements on each edge. The results were obtained up to an accuracy of 3%.

4. INTRODUCTION FOR USING FLUENT AND GAMBIT

4.1 GAMBIT

GAMBIT is geometry and mesh generation software for computational fluid dynamics (CFD) analysis. GAMBIT has a single interface for geometry creation, meshing, assigning zone types and that brings together several preprocessing technologies in one environment. GAMBIT receives the user input by means of a graphics user interface (GUI). The main steps for using GAMBIT are:

- Creating the geometry

- Meshing the geometry

- Assigning appropriate zones

The details of each of the above steps have been discussed in the following sections. Further details of each one of them have been discussed in GAMBIT's user guide [17].

4.1.1 Creating Geometry

A bottom up approach has been used in creating the geometry in this problem. First the vertices have been created at the required locations using the GUI by specifying the coordinates of each vertex. All the vertices created are in the Z=0 plane. Next, the created vertices were joined using edges. Thus a two-dimensional elbow was formed in the Z=0 plane. After joining the edges circular edges were created at the inlet and the outlet using the center and the end points. Now, after creating all the edges, the symmetric face, inlet face and outlet face were created by directly joining the edges. The

wall face is created by sweeping the circular edge at the inlet along the axis of the elbow. Thus, after forming all the four faces the volume has been created by "stitching" all the faces together.

4.1.2 Meshing the Model

As geometry has been created the next step is to mesh the geometry. The main meshing options available in GAMBIT are:

- Boundary Layer Mesh

- Edge mesh

- Face mesh

- Volume mesh

- Group mesh

4.1.2.1 Boundary Layer Mesh

Boundary layer mesh defines the spacing of the mesh node rows near the edges or faces. As the velocity gradients are very high near the boundary a high density mesh is required near the boundary. They are mainly used to control the mesh density and hence, the amount of information available from the computational model. To define the boundary layer, one must specify the following information:

- Boundary-layer algorithm

- Height of first row

- Growth factor

- Total number of rows

- Edge or face to which boundary layer is attached

- Direction of the boundary layer

4.1.2.2 Edge Mesh

The "Mesh Edges" operation grades or meshes any or all the edges in the model. When you grade an edge, GAMBIT applies the mesh node spacing specifications but does not create mesh nodes on the edge. The different options available in the "Mesh Edges" menu are edge mesh, edge modify, edge picklink, edge pickunlink commands. To perform a grading or meshing operation, you must specify the following parameters:

- Edges to which the grading specifications apply

- Grading scheme

- Mesh node spacing (number of intervals)

- Edge meshing options

4.1.2.3 Face Mesh

The Mesh Faces operation creates the mesh for one or more faces in the model. When you mesh a face, GAMBIT creates mesh nodes on the face according to the currently specified meshing parameters. The different options available in the "Mesh Faces" operation are 'face mesh' and 'face modify' commands. The Mesh Faces operation requires the following input parameters:

- Faces to be meshed

- Meshing scheme

- Mesh node spacing

- Face meshing options

4.1.2.4 Volume Mesh

The Mesh Volumes operation creates a mesh for one or more volumes in the model. When you mesh a volume, GAMBIT creates mesh nodes throughout the volume according to the currently specified meshing parameters. The "Mesh Volume" operation consists of volume mesh and volume modify commands. To mesh a volume, one must specify the following parameters:

- Volumes to be meshed

- Meshing scheme

- Mesh node spacing

- Meshing options

4.1.2.5 Mesh Groups

The Mesh Groups operation activates meshing operations for one or more groups of topological entities. When you mesh a group by means of the Mesh Groups command, GAMBIT performs meshing operations for all of the topological entities that comprise components of the group. If you apply meshing parameters to any or all

components of the group prior to executing the Mesh groups command, GAMBIT meshes those components according to their previously applied parameters. All other components of the group are meshed according to the default meshing parameters. For example, if you mesh a group that includes three edges to one of which has been previously applied a double-sided, successive-ratio grading scheme, GAMBIT honors the applied scheme when it meshes the group but meshes the other two edges according to the current default grading scheme. To perform a group meshing operation, you must specify the following parameters:

- Group names

- Mesh node spacing

The group names parameter specifies the name of one or more existing groups the components of which are to be meshed. The mesh node spacing parameter specifies the number of edge mesh intervals that are to be created on all edges for which a grading scheme has not been previously applied.

4.1.3 GAMBIT Procedure for Elbow Geometry

In the case that is being dealt with the next step is to mesh the geometry. For this, the edges need to be meshed first by specifying the type of grading that needs to be used, the interval count and the ratio of the successive elements. For meshing the edges at the inlet and outlet faces a "successive ratio" grading was used with the ratio as 1.0. The interval count was specified to be 30 on each edge. The edge that was meshed is the edge along the axis of the elbow. For this, the grading type used was "Bell shaped" with

a ratio of 0.4 and interval count specified was 130. Bell shaped type was chosen in order to get a high density of the mesh at the bend. Now, after creating the mesh on the edges the "Boundary layer mesh" was created on the inlet and outlet faces. The properties of the boundary layer were: height of the first row was 0.0003 units, growth factor was 1.1 and the number of rows was specified to be 7 resulting in the boundary layer which was 0.0028 units deep. Along with the other properties the edge to which boundary layer was attached and the direction of the boundary layer were also specified. The next step is to mesh the faces of the geometry. The quadrilateral elements were used to mesh the faces and the type chosen was "Map". The interval size was chosen to be 1 (default). The faces to be meshed were selected. Now after meshing the faces next step is to mesh the volume. Hexagonal elements were used to mesh the volume and the type of mesh chosen was "Map". The interval size chosen was 1 (default). The face meshed was swept along the axis of the elbow to create the volume mesh. Now, after the meshing is done one needs check for the quality of mesh and modify it if needed. The different ways of checking the grid is to check the aspect ratio of all the cells or even the equi angle skew can be checked.

4.1.4 Specifying the Zones

After meshing the geometry the next step is to assign the zone types for the boundaries. Zone-type specifications define the physical and operational characteristics of the model at its boundaries and within specific regions of its domain. There are two classes of zone-type specifications:

- Boundary types

- Continuum types

Boundary-type specifications, such as WALL or SYMMETRY, define the characteristics of the model at its external or internal boundaries. Continuum-type specifications, such as FLUID or SOLID, define the characteristics of the model within specified regions of its domain. Boundary-type specifications define the physical and operational characteristics of the model at those topological entities that represent model boundaries. For example, if you assign an INFLOW boundary type specification to a face entity that is part of three-dimensional model, the model is defined such that material flows into the model domain through the specified face. Likewise, if you specify a SYMMETRY boundary type to an edge entity that is part of a two-dimensional model, the model is defined such that flow, temperature, and pressure gradients are identically zero along the specified edge. As a result, physical conditions in the regions immediately adjacent to either side of the edge are identical to each other.

Continuum-type specifications define the physical characteristics of the model within specified regions of its domain. For example, if you assign a FLUID continuum-type specification to a volume entity, the model is defined such that equations of momentum, continuity, and species transport apply at mesh nodes or cells that exist within the volume. Conversely, if you assign a SOLID continuum-type specification to a volume entity, only the energy and species transport equations (without convection) apply at the mesh nodes or cells that exist within the volume.

In the present geometry we need to specify four boundary conditions and one continuum condition. Since we have four different faces bounding the volume we need to assign four different boundary conditions to the faces. The zones specified were, velocity inlet for the inlet face, Wall condition for surface of the elbow, pressure outlet for the outlet face, symmetry condition for the Z=0 face. The continuum was specified to be a fluid.

4.2 FLUENT

4.2.1 Introduction

Once the geometry is meshed in GAMBIT the next step is to import the mesh file into FLUENT and the subsequent operations are all performed in FLUENT. The details of FLUENT have been discussed in this section using FLUENT's user guide as a reference [18]. The operations performed in FLUENT include grid check, assigning boundary conditions, defining material properties, compiling the user defined function, executing the solution, finding grid independent solution and refining the mesh, viewing and post processing results. Before we go into the details of the problem we will just skim through the some basic fundamentals required for using FLUENT.

FLUENT is a computer program for modeling fluid flow and heat transfer in different geometries. FLUENT provides mesh flexibility, including the ability to solve flow problems using unstructured meshes that can be generated about complex geometries with relative ease. Supported mesh types include 2D triangular or quadrilateral, 3D   tetrahedral or hexahedral or pyramid or wedge or polyhedral, and

mixed (hybrid) meshes. FLUENT also allows us to refine or coarsen the grid based on the flow solution. FLUENT is written in the computer language C and makes use of the flexibility and variety offered by the language. Hence, dynamic memory allocation, efficient data structures, and flexible solver control are all possible. In addition, FLUENT uses a client architecture, which allows it to run simultaneously on different desktop workstations by interacting with each other. FLUENT package consists of FLUENT which is the solver, next it has GAMBIT, the preprocessor for geometry modeling and mesh generation, it also has TGrid which acts as an additional preprocessor that can generate volume meshes from existing boundary meshes, finally it also has filters used to import surface and volume meshes from CAD/CAE packages such as ANSYS. The figure 4.1 below shows the structure of the FLUENT package.

```
GAMBIT
  • Model geometry
  • 2D/3D mesh
```

```
Other CAD/CAE
packages
```

Geometry/mesh

Geometry mesh

Boundary or
volume mesh

Mesh

```
FLUENT
  • Mesh import
  • Physical models
  • Boundary conditions
  • Material properties
  • Calculation
  • Post processing
```

```
TGRID
  • 2D triangular mesh
  • 3D tetrahedral mesh
  • 2D or 3D hybrid
```

Mesh

Mesh
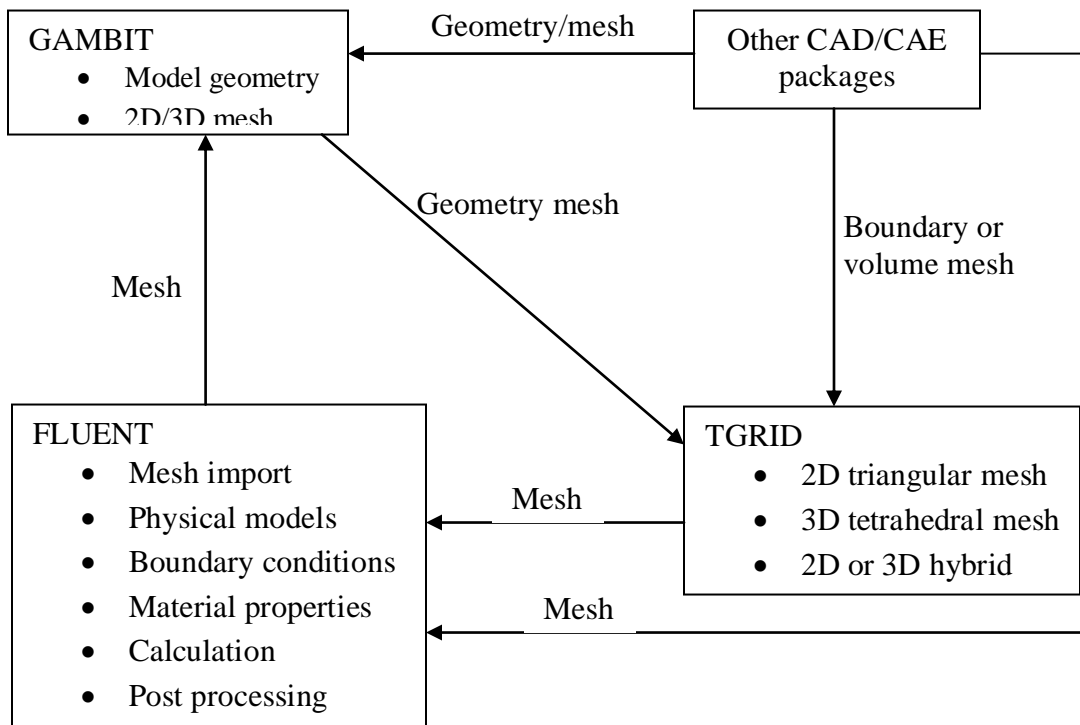
Figure 4.1 Structure of FLUENT package

Once important features of the problem have been determined, one needs to follow these steps in order to solve any problem using FLUENT

- Define the modeling goals.

- Create the model geometry and grid. (done in GAMBIT)

- Set up the solver and physical models.

- Compute and monitor the solution.

- Examine and save the results.

- Consider revisions to the numerical or physical model parameters, if necessary.

4.2.2 Grid Check

After creating the geometry and meshing the geometry in GAMBIT the first step that needs to done in FLUENT is the "Grid check". The grid checking capability in FLUENT provides domain extents, volume statistics, grid topology and periodic boundary information, verification of simplex counters, and (for axisymmetric cases) node position verification with respect to the x axis. It is generally a good idea to check your grid right after reading it into the solver, in order to detect any grid trouble before you get started with the problem setup.

4.2.3 Boundary Conditions

Boundary conditions specify the flow and thermal variables on the boundaries of your physical model. They are, therefore, a critical component of your FLUENT simulations and it is important that they are specified appropriately. The boundary types available in FLUENT are classified as follows:

- Flow inlet and exit boundaries: pressure inlet, velocity inlet, mass flow inlet, inlet vent, intake fan, pressure outlet, pressure far-field, outflow, outlet vent, and exhaust fan.

- Wall, repeating, and pole boundaries: wall, symmetry, periodic, and axis.

- Internal cell zones: fluid, and solid (porous is a type of fluid zone).

- Internal face boundaries: fan, radiator, porous jump, wall, and interior.

In the problem we are dealing with right now the boundary conditions that have been used are velocity inlet, pressure outlet, wall and symmetry. Now we will be going into the details of these boundary conditions.

4.2.3.1 Velocity Inlet Boundary Condition

Velocity inlet boundary conditions are used to define the flow velocity, along with all relevant scalar properties of the flow, at flow inlets. The total (stagnation) properties of the flow are not fixed, so they will rise to whatever value is necessary to provide the prescribed velocity distribution. This boundary condition is intended for incompressible flows, and its use in compressible flows will lead to a nonphysical result. You need to enter the velocity magnitude and the direction or velocity components for the velocity inlet boundary condition. If you are going to set the velocity magnitude and direction or the velocity components, and your geometry is 3D, you will next choose the coordinate system in which you will define the vector or velocity components. Choose Cartesian (X, Y, Z), Cylindrical (Radial, Tangential, Axial), or Local Cylindrical (Radial, Tangential, Axial) in the Coordinate System drop-down list.

4.2.3.2 Pressure Outlet Boundary Condition

Pressure outlet boundary conditions require the specification of a static (gauge) pressure at the outlet boundary. The value of the specified static pressure is used only while the flow is subsonic. Should the flow become locally supersonic, the specified pressure will no longer be used; pressure will be extrapolated from the flow in the

interior. All other flow quantities are extrapolated from the interior. A set of "backflow" conditions is also specified should the flow reverse direction at the pressure outlet boundary during the solution process. Convergence difficulties will be minimized if you specify realistic values for the backflow quantities. Several options in FLUENT exist, where a radial equilibrium outlet boundary condition can be used, and a target mass flow rate for pressure outlets can be specified.

4.2.3.3 Wall Boundary Condition

Wall boundary condition is used to bound the fluid and solid regions. In viscous flows, no-slip boundary condition is enforced at walls by default, but you can specify a tangential velocity component in terms of the translational or rotational motion of the wall boundary, or model a "slip" wall by specifying shear. You can also model a slip wall with zero shear using the symmetry boundary type, but using a symmetry boundary will apply symmetry conditions for all equations. The shear stress and heat transfer between the fluid and wall are computed based on the flow details in the local flow field.

4.2.3.4 Shear Stress Calculation at the Wall

For no-slip wall conditions, FLUENT uses the properties of the flow adjacent to the wall/fluid boundary to predict the shear stress on the fluid at the wall. In laminar flows this calculation simply depends on the velocity gradient at the wall. For specified-shear walls, FLUENT will compute the tangential velocity at the boundary. If you are

modeling inviscid flow with FLUENT, all walls use a slip condition, so they are frictionless and exert no shear stress on the adjacent fluid.

In a laminar flow, the wall shear stress is defined by the normal velocity gradient at the wall as,

$$\tau_w = \mu \left(\frac{\partial v}{\partial n}\right)$$

When there is a steep velocity gradient at the wall, you must be sure that the grid is sufficiently fine to accurately resolve the boundary layer.

4.2.3.5 Symmetry Boundary Condition

Symmetry boundary conditions are used when the physical geometry of interest, and the expected pattern of the flow/thermal solution, have mirror symmetry. They can also be used to model zero-shear slip walls in viscous flows. You do not define any boundary conditions at symmetry boundaries, but you must take care to correctly define your symmetry boundary locations.

FLUENT assumes a zero flux of all quantities across a symmetry boundary. There is no convective flux across a symmetry plane: the normal velocity component at the symmetry plane is thus zero. There is no diffusion flux across a symmetry plane: the normal gradients of all flow variables are thus zero at the symmetry plane. The symmetry boundary condition can therefore be summarized as follows:

* zero normal velocity at a symmetry plane

* zero normal gradients of all variables at a symmetry plane

As stated above, these conditions determine a zero flux across the symmetry plane, which is required by the definition of symmetry. Since the shear stress is zero at a symmetry boundary, it can also be interpreted as a "slip" wall when used in viscous flow calculations.

4.2.3.6 Fluid Continuum Condition

A fluid zone is a group of cells for which all active equations are solved. The only required input for a fluid zone is the type of fluid material. You must indicate which material the fluid zone contains so that the appropriate material properties will be used. To define the material contained in the fluid zone, select the appropriate item in the Material Name drop-down list. This list will contain all fluid materials that have been defined (or loaded from the materials database) in the Materials panel.

4.2.4 Defining Materials

An important step in the setup of the model is to define the materials and their physical properties. Material properties are defined in the Materials panel, where you can enter values for the properties that are relevant to the problem scope you have defined in the Models panel. These properties may include the following:

density and/or molecular weights

- viscosity

- heat capacity

- thermal conductivity

- UDS diffusion coefficients

- mass diffusion coefficients

- standard state enthalpies

- kinetic theory parameters

Properties may be temperature-dependent and/or composition-dependent, with temperature dependence based on a polynomial, piecewise-linear, or piecewise-polynomial function and individual component properties either defined by you or computed via kinetic theory. The main property of the fluid we will looking into is the viscosity. Hence we will now see the details about the viscosity function in FLUENT. FLUENT provides several options for definition of the fluid viscosity:

- constant viscosity

- temperature dependent and/or composition dependent viscosity

- kinetic theory

- non-Newtonian viscosity

- user-defined function

FLUENT provides four options for modeling non-Newtonian flows:

- power law

- Carreau model for pseudo-plastics

- Cross model

- Herschel-Bulkley model for Bingham plastics

4.2.5 Solvers

FLUENT allows you to choose one of the two numerical methods:

- pressure-based solver

- density-based solver

Historically speaking, the pressure-based approach was developed for low-speed incompressible flows, while the density-based approach was mainly used for high-speed compressible flows. However, recently both methods have been extended and reformulated to solve and operate for a wide range of flow conditions beyond their traditional or original intent.

In both methods the velocity field is obtained from the momentum equations. In the density-based approach, the continuity equation is used to obtain the density field while the pressure field is determined from the equation of state. On the other hand, in the pressure-based approach, the pressure field is extracted by solving a pressure or pressure correction equation which is obtained by manipulating continuity and momentum equations.

Using either method, FLUENT will solve the governing integral equations for the conservation of mass and momentum, and (when appropriate) for energy and other scalars such as turbulence and chemical species. In both cases a control-volume-based technique is used that consists of:

- Division of the domain into discrete control volumes using a computational grid.

- Integration of the governing equations on the individual control volumes to construct algebraic equations for the discrete dependent variables ("unknowns") such as velocities, pressure, temperature, and conserved scalars.

- Linearization of the discretized equations and solution of the resultant linear equation system to yield updated values of the dependent variables. The two numerical methods employ a similar discretization process (finite-volume), but the approach used to linearize and solve the discretized equations is different.

4.2.5.1 Pressure Based Solver

The pressure-based solver employs an algorithm which belongs to a general class of methods called the projection method. In the projection method, wherein the constraint of mass conservation (continuity) of the velocity field is achieved by solving a pressure (or pressure correction) equation. The pressure equation is derived from the continuity and the momentum equations in such a way that the velocity field, corrected by the pressure, satisfies the continuity. Since the governing equations are nonlinear and coupled to one another, the solution process involves iterations wherein the entire set of governing equations is solved repeatedly until the solution converges. Two pressure-based solver algorithms are available in FLUENT. A segregated algorithm, and a coupled algorithm.

The pressure-based solver uses a solution algorithm where the governing equations are solved sequentially (i.e., segregated from one another). Because the governing equations are non-linear and coupled, the solution loop must be carried out

iteratively in order to obtain a converged numerical solution. In the segregated algorithm, the individual governing equations for the solution variables are solved one after another. Each governing equation, while being solved, is "decoupled" or "segregated" from other equations, hence its name. The segregated algorithm is memory-efficient, since the discretized equations need only be stored in the memory one at a time. However, the solution convergence is relatively slow,as the equations are solved in a decoupled manner. With the segregated algorithm, each iteration consists of the steps outlined below:

1. Update fluid properties (e,g, density, viscosity, specific heat) based on the current solution.

2. Solve the momentum equations, one after another, using the recently updated values of pressure and face mass fluxes.

3. Solve the pressure correction equation using the recently obtained velocity field and the mass-flux.

4. Correct face mass fluxes, pressure, and the velocity field using the pressure correction obtained from Step 3.

5. Solve the equations for additional scalars, if any, such as turbulent quantities, energy, species, and radiation intensity using the current values of the solution variables.

6. Update the source terms arising from the interactions among different phases (e.g., source term for the carrier phase due to discrete particles).

7. Check for the convergence of the equations.

These steps are continued until the convergence criteria are met. The basic steps to followed for using the solver are:

1. Choose the discretization scheme and, for the pressure-based solver, the pressure interpolation scheme.

2. (pressure-based solver only) Select the pressure-velocity coupling method.

3. (pressure-based solver only) Select the porous media velocity method.

4. Select how you want the derivatives to be evaluated by choosing a gradient option.

5. Set the under-relaxation factors.

6. Make any additional modifications to the solver settings that are suggested in the chapters or sections that describe the models you are using.

7. Initialize the solution.

8. Enable the appropriate solution monitors.

9. Start calculating.

4.2.6 Initializing the Solution

Before starting your CFD simulation, you must provide FLUENT with an initial "guess" for the solution flow field. In many cases, you must take extra care to provide an initial solution that will allow the desired final solution to be attained. A real-life supersonic wind tunnel, for example, will not "start" if the back pressure is simply lowered to its operating value; the flow will choke at the tunnel throat and will not transition to supersonic. The same holds true for a numerical simulation: the flow must

be initialized to a supersonic flow or it will simply choke and remain subsonic.There are two methods for initializing the solution:

- Initialize the entire flow field (in all cells).

- Patch values or functions for selected flow variables in selected cell zones or "registers" of cells. (Registers are created with the same functions that are used to mark cells for adaption.)

4.2.7 Monitoring Solution Convergence

During the solution process you can monitor the convergence dynamically by checking residuals, statistics, force values, surface integrals, and volume integrals. You can print reports of or display plots of lift, drag, and moment coefficients, surface integrations, and residuals for the solution variables. For unsteady flows, you can also monitor elapsed time.

4.2.8 Under-relaxation and Over-relaxation

In an iterative solution of the algebraic equations or in the overall iterative scheme for handling nonlinearity it is often desirable to speed up or to slow down the changes from iteration to iteration, in the values of the dependent variable. This process is called over-relaxation or under-relaxation, depending on whether the changes are accelerated or slowed down. With the line-by-line method being the most common one used for solving the nonlinear equations, the use of over-relaxation is less common.

Under-relaxation is a very useful device for nonlinear problems. It is often employed to avoid divergence in the iterative solution of highly nonlinear equations.

Because of the nonlinearity of the equation set being solved by FLUENT, it is necessary to control the change of the variable. This is typically achieved by under-relaxation of variables (also referred to as explicit relaxation), which reduces the change of the variable produced during each iteration.

The under-relaxation of equations, also known as implicit relaxation, is used in the pressure-based solver to stabilize the convergence behavior of the outer nonlinear iterations by introducing selective amounts of the change in the system of discretized equations.

When the relaxation factor is between 0 and 1 its effect is under-relaxation; that is the new value of the variable stays closer to the old value. For a very small α, the changes in the variable become very slow . When α is greater than 1, over-relaxation is produced. There are no general rules for choosing the best value of α. The optimum value depends on number of factors such as the nature of the problem, number of grid points, the grid spacing, and the iterative procedure used.

4.2.9 User Defined Functions

A user-defined function, or UDF, is a function that you program that can be dynamically loaded with the FLUENT solver to enhance the standard features of the code. For example, you can use a UDF to define your own boundary conditions, material properties, and source terms for your flow regime, as well as specify customized model

parameters (e.g., DPM, multiphase models), initialize a solution, or enhance post-processing.

UDFs are written in the C programming language using any text editor and the source code file is saved with a .c extension (e.g., udf.c). One source file can contain a single UDF or multiple UDFs, and you can define multiple source files.

UDFs are defined using DEFINE macros provided by FLUENT Inc. They are coded using additional macros and functions also supplied by FLUENT Inc. that access FLUENT solver data and perform other tasks.

Every UDF must contain the udf.h file inclusion directive (#include "udf.h") at the beginning of the source code file, which allows definitions of DEFINE macros and other FLUENT-provided macros and functions to be included during the compilation process. Note that values that are passed to a solver by a UDF or returned by the solver to a UDF are specified in SI units.

Source files containing UDFs can be either interpreted or compiled in FLUENT. For interpreted UDFs, source files are interpreted and loaded directly at runtime, in a single-step process. For compiled UDFs, the process involves two separate steps. A shared object code library is first built and then it is loaded into FLUENT. Once interpreted or compiled, UDFs will become visible and selectable in FLUENT graphics panels, and can be hooked to a solver by choosing the function name in the appropriate panel.

In summary, UDFs:

- are written in the C programming language.

- must have an include statement for the udf.h file.

- must be defined using DEFINE macros supplied by FLUENT Inc.

- utilize predefined macros and functions supplied by FLUENT Inc. to acccess FLUENT solver data and perform other tasks.

- are executed as interpreted or compiled functions.

- are hooked to a FLUENT solver using a graphical user interface panel.

- use and return values specified in SI units.

4.2.10 Discretization

The discretization option in the solution controls contains the option to choose discretization method for the convective terms of each governing equation while second-order accuracy is automatically used for the viscous terms. The discretization schemes available for the pressure equation are Standard, Presto, Linear, Second Order, and Body Force Weighted. The discretization schemes available for the momentum equation are First Order Upwind, Second Order Upwind, Power Law, QUICK, or Third-Order MUSCL. The details of all the discretization schemes have been discussed by Patankar [19].

4.2.11 Pressure Velocity Coupling

The pressure-based solver helps to solve the flow problem in either a segregated or coupled manner. FLUENT provides the option to choose among five pressure-velocity coupling algorithms: SIMPLE, SIMPLEC, PISO, Coupled, and (for unsteady

flows using the non-iterative time advancement scheme (NITA)) Fractional Step (FSM). SIMPLE, SIMPLEC, PISO, and Fractional Step use the pressure-based segregated algorithm, while Coupled uses the pressure-based coupled solver.

In FLUENT, both the standard SIMPLE algorithm and the SIMPLEC (SIMPLE-Consistent) algorithm are available. SIMPLE is the default, but many problems will benefit from using SIMPLEC, particularly because of the increased under-relaxation that can be applied, as described below.

For relatively uncomplicated problems (laminar flows with no additional models activated) in which convergence is limited by the pressure-velocity coupling, you can often obtain a converged solution more quickly using SIMPLEC. With SIMPLEC, the pressure-correction under-relaxation factor is generally set to 1.0, which aids in convergence speed-up. For complicated flows involving turbulence and/or additional physical models, SIMPLEC will improve convergence only if it is being limited by the pressure-velocity coupling. Often it will be one of the additional modeling parameters that limits convergence; in this case, SIMPLE and SIMPLEC will give similar convergence rates. In the present problem a SIMPLE algorithm has been used for the pressure velocity coupling.

4.2.12 FLUENT Procedure for the Elbow Geometry

First, the model geometry and mesh created in GAMBIT (.msh file) is imported into FLUENT. Then the geometry is checked for the grid. After the grid check is done the grid created is now ready to be used for the computations. The next step is to set all

the variables such as temperature, pressure, velocity to the SI units. Next, the boundary conditions for the model should be assigned. The boundary conditions used for the circular inlet and outlet faces are velocity inlet and the pressure outlet respectively. Then the boundary condition assigned to the $Z=0$ plane is a symmetry boundary condition and the wall boundary condition is set to the circular face along the axis of the elbow. The continuum condition also needs to be specified along with the boundary conditions. The continuum type was selected to be a fluid and the fluid type was selected from the list of materials which includes all the properties of the fluid such as density, viscosity, thermal conductivity, diffusivity. There a quite a few data that needs to be specified for assigning each type of boundary condition. First, for the velocity inlet boundary condition at the inlet face a Cartesian (X, Y, Z) co-ordinate system has been chosen and the velocity components were specified along the three directions. These velocities were calculated from the Reynolds number relationship which has been previously discussed. This velocity inlet boundary condition is mainly useful for incompressible flows. Next, at the outlet face a pressure outlet boundary condition has been specified. The outlet has been assumed to be at the atmospheric pressure and hence the static gauge pressure was specified to be zero and the backflow direction was specified to be normal to the boundary. Next, the symmetry condition was specified at the $Z=0$ plane. There are no additional inputs required for this boundary condition. The last boundary is the wall condition specified at the face of the pipe. The wall is specified to be a stationary one and a no slip shear condition is specified at the wall. After specifying the boundary conditions the next step is to specify the materials. The materials required for the

problem is created in the materials panel by specifying different properties such as density, viscosity, thermal diffusivity, thermal conductivity. All the properties except for viscosity were specified to be a constant and viscosity has been defined to be a user defined function. When the viscosity is specified to be a user defined function a pop-up comes showing all the user defined functions that have been compiled. The user defined function which is written using C-programming returns the value of viscosity after each iteration, evaluated from the velocity gradients computed from the iteration. The viscosity obtained from the iteration is used as an input to the next iteration. The viscosity user defined function is compiled as an interpreted UDF. Along with the UDF the solver has also been specified. A pressure based solver was chosen for the analysis with an implicit formulation. The problem chosen is a 3D and steady state problem. Velocity formulation was chosen to be absolute. Now, after assigning the solver controls the solution controls need to be taken care of for finding the solution of the problem. Since the problem does not involve the temperature only the flow equations need to be solved. The pressure velocity coupling is obtained by using a SIMPLE algorithm. The discretization of the convective terms in the pressure and momentum equations were done using a standard and power law schemes. A power law scheme was used since it was found to be more accurate than the remaining ones. The pressure and momentum equations were solved using under relaxation and the under relaxation factors used were 0.3 and 0.5 for the pressure and momentum equations respectively. Next, after setting up the solution controls the solution variables need to be initialized i.e a guess value was chosen which finally converges to the solution. The initial guess value of (p, u, v, w)

were chosen to be $(0, 0, 0, 0)$. The solution has been monitored using the residual values as the monitors. The residual values were set to 10^{-5} for the X-velocity, Y-velocity, Z-velocity and the continuity equation. When these residual values have been obtained the solution is said to be converged. The residuals have been plotted during the iterative process and they were observed to die down with the increase in the number of iterations. Now, after setting the initial guess value and the monitor for checking the convergence the iterations are ready to be carried out. After obtaining the convergence the velocity profiles can be obtained. The simulations have been done for two Reynolds numbers, three different geometries and five power law index values which includes shear-thickening, Newtonian and shear-thinning fluids. The results obtained have been interpreted and the post processing is done. After obtaining the first set of results the next step is to check the grid independence of the results obtained. This is done by increasing the mesh size and the corresponding change in the variable values measured. The results are said to be grid independent if the results obtained by increasing the grid size are within an error of 3%.

The viscosity user defined function which was written using C-programming is as follows:

#include "udf.h"

#define index 0.9

#define alph 1.00

#define mu 0.00384

DEFINE_PROPERTY(material_property,cell,thread)

```
{

  float trace;

  double visc;

  float u[3], v[3], w[3];

  int j;

  for(j=0;j<3;j++)

  {

      u[j]=C_U_G(cell,thread)[j];

      v[j]=C_V_G(cell,thread)[j];

      w[j]=C_W_G(cell,thread)[j];

  }

trace=0.5*(2*pow(u[0],2)+pow(v[0]+u[1],2)+2*pow(v[1],2)+pow(v[2]+w[1],2)+2*pow

(w[2],2)+pow(w[0]+u[2],2));

visc=mu*pow(1+alph*trace,(index-1)/2);

return visc;

}
```

5. RESULTS AND CONCLUSIONS

The residuals of the flow variables have all dropped down to 10^{-5} after performing the required number of iterations. After obtaining the convergence the next step is the post processing of the results obtained. The different values of variables considered for the simulations are, power law index, n=0.60, 0.75, 0.90, 1.00, 1.35, 1.45, 1.55 and two Reynolds numbers, Re=200, 1100. The non-dimensional geometry parameter considered is N= 0.7, 1.0, 5.0. So a total of 42 cases were simulated. The issues that have been covered in this section are:

- Contour of magnitude of velocity in the plane of symmetry.

- The nature of the secondary flow in the elbow is discussed for different parametric values. The section that has been chosen is the elbow midsection that is at an angle of 45° in the elbow bend.

- Variation of the Wall stress has been studied for the different cases considered.

The variation of all these properties with the power law index, Reynolds number and aspect ratio has been considered.

First we will look into the variation of velocity contours with different parameters. Figure 5.1 shows the velocity contours for the case n=0.6, Re=200, N=0.7 and figure 5.2 shows the case for same values of n, N and Re=1100.
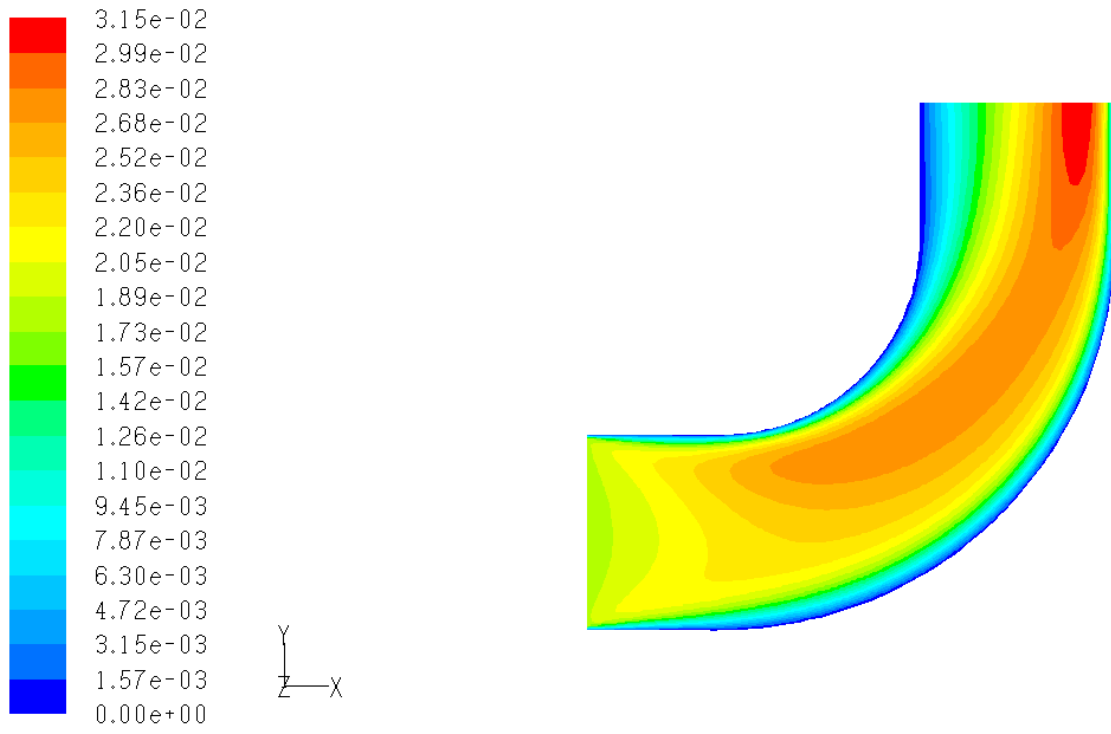
Figure 5.1 Contours of magnitude of velocity for n=0.6, N=0.7, Re=200 in the

plane of symmetry
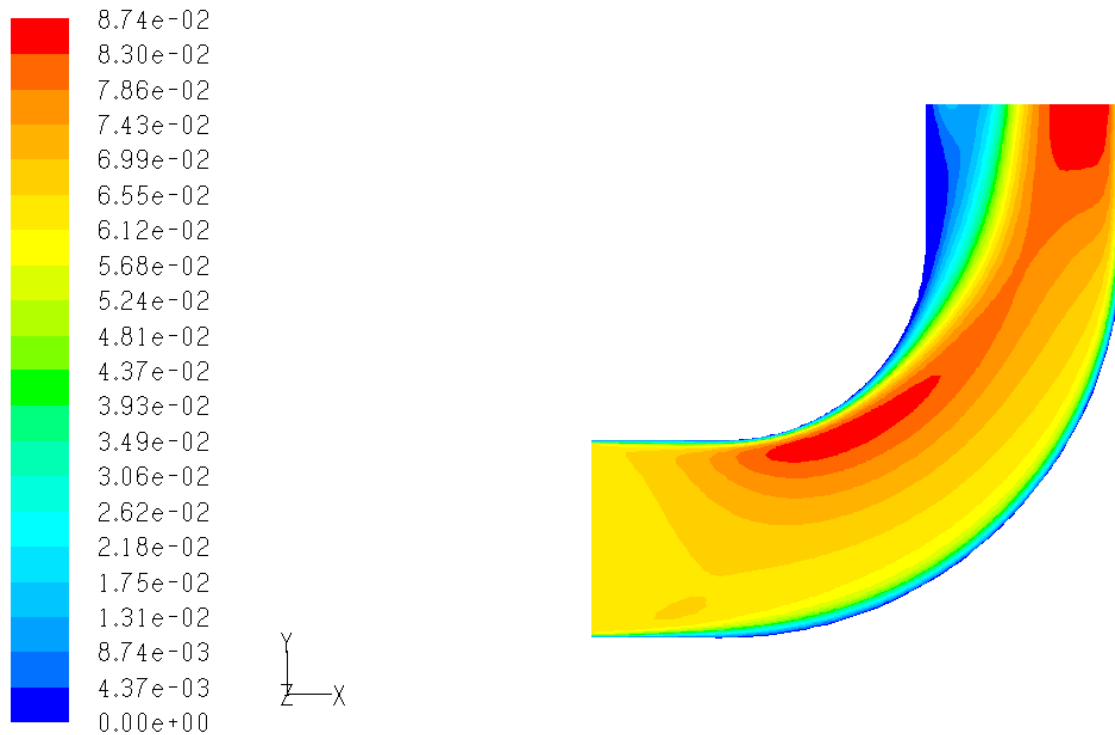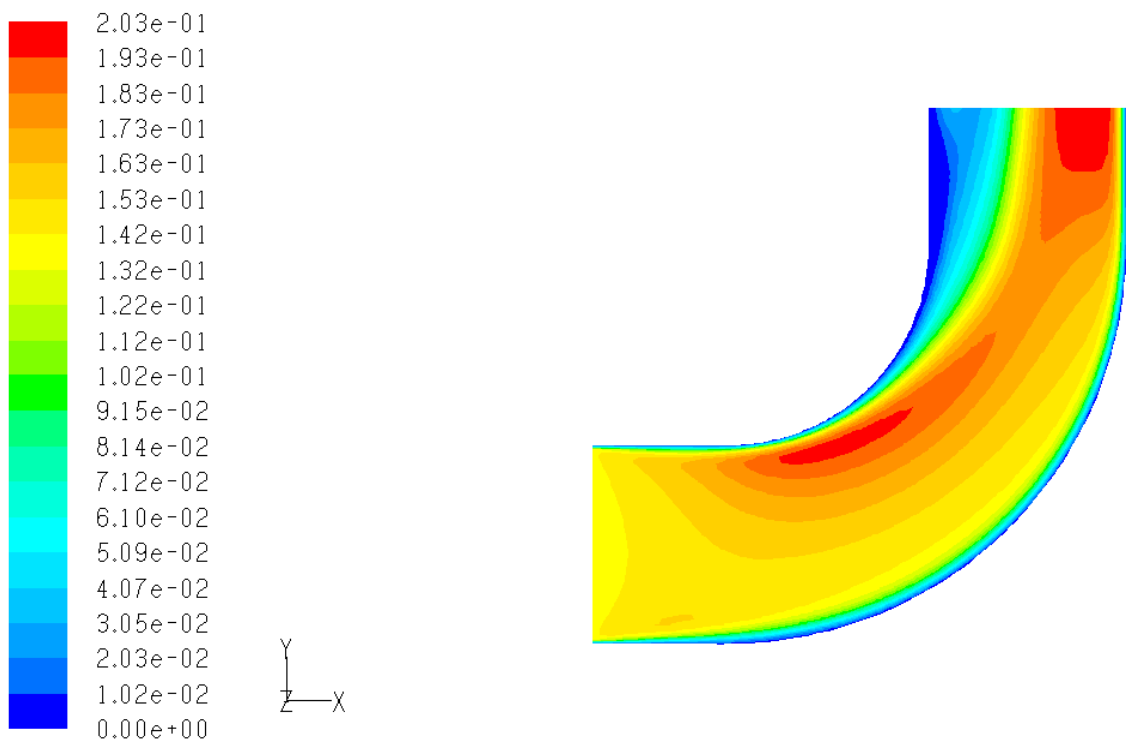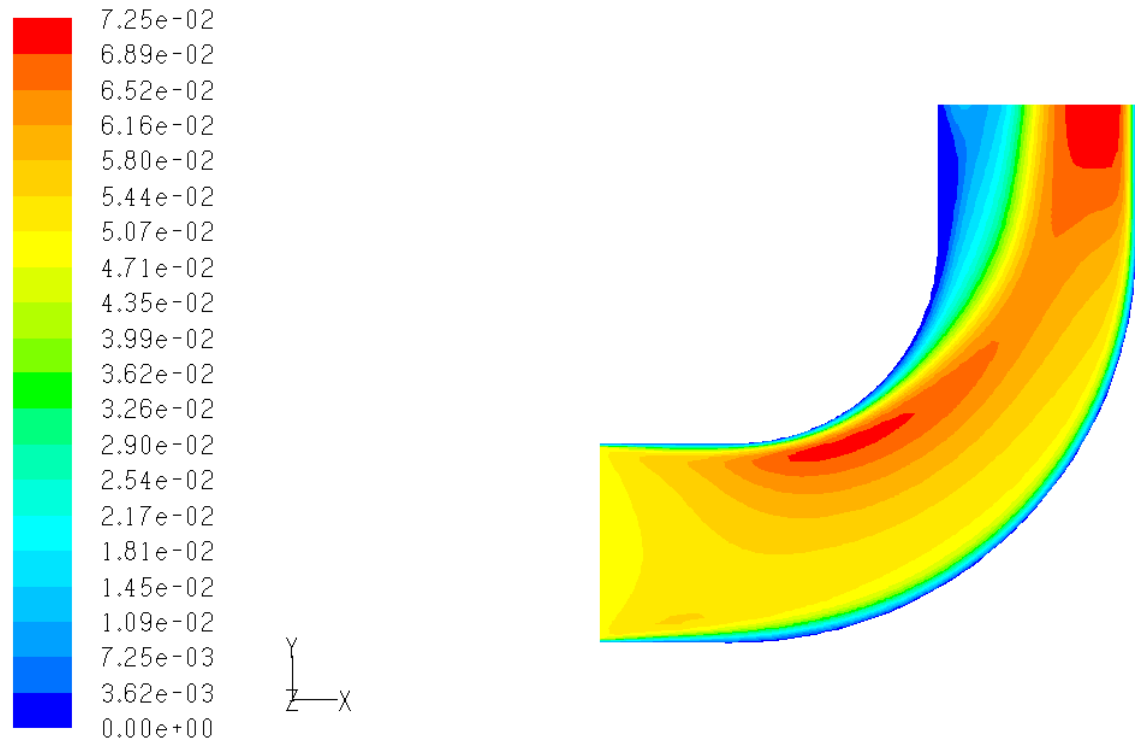
Figure 5.2 Contours of magnitude of velocity for n=0.6, N=0.7, Re=1100 in the plane of

symmetry

The above two figures show the variation of profiles caused by the variation in

the Reynolds number with constant power law index and aspect ratio. The above cases

are both for a shear thinning fluid. It can be concluded from the two contours that as the

Reynolds number is increased it causes the development of the recirculation zone near

the inner radius of the elbow. For both the cases the fluid in the elbow has the maximum

velocity at the exit in the outer part of the elbow. These two patterns were found in all

the values of power law index considered for N=0.7.

Figure 5.3 Contours of magnitude of velocity for n=0.9, N=0.7, Re=1100 in the plane of

symmetry

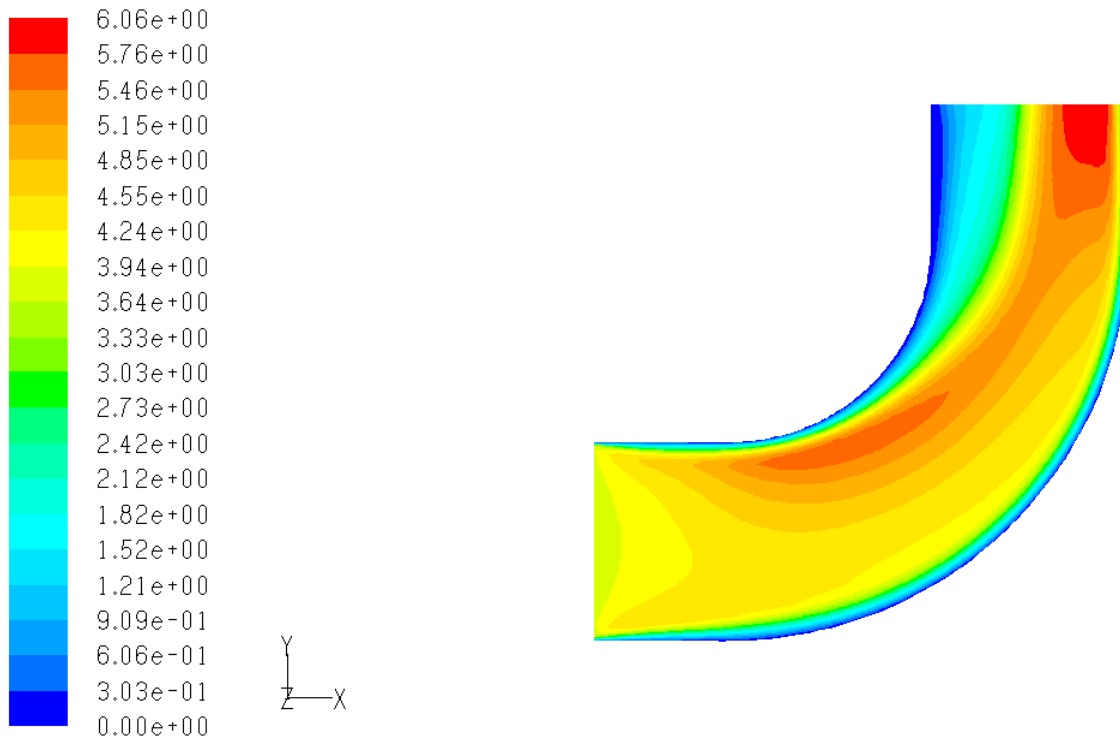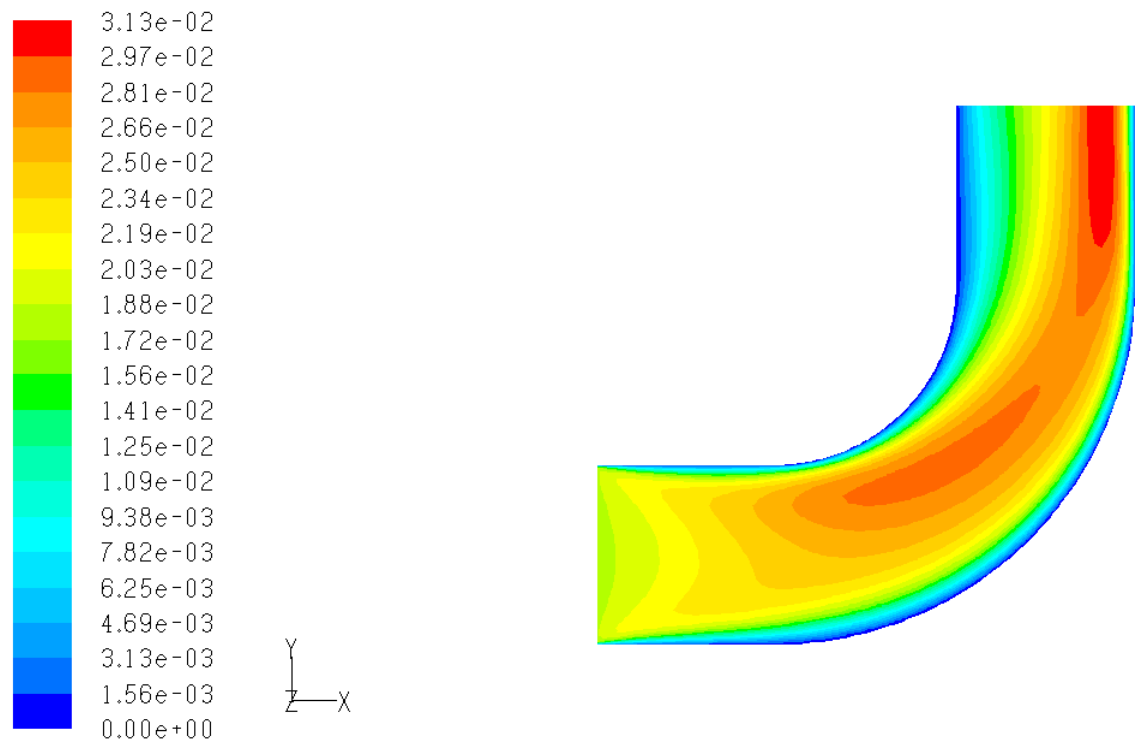Figure 5.4 Contours of magnitude of velocity for n=1.0, N=0.7, Re=1100 in the plane of

symmetry

Figure 5.5 Contours of magnitude of velocity for n=1.55, N=0.7, Re=1100 in the plane

of symmetry

From the figure 5.2-5.5 it can be seen how the velocity profiles vary with the variation of the power law index of the fluid. The amount of the recirculation slowly decreases as the liquid becomes thicker. That is, the shear thickening fluid has lesser recirculation region and the flow is much smoother than compared to that of shear thinning fluid. In addition, the velocity of the fluid at the recirculation zone is much lesser compared to the maximum velocity reached in case of the shear thickening fluid.

3.13e-02
2.97e-02
2.81e-02
2.66e-02
2.50e-02
2.34e-02
2.19e-02
2.03e-02
1.88e-02
1.72e-02
1.56e-02
1.41e-02
1.25e-02
1.09e-02
9.38e-03
7.82e-03
6.25e-03
4.69e-03
3.13e-03
1.56e-03
0.00e+00

Figure 5.6 Contours of magnitude of velocity for n=0.6, N=1.0, Re=200 in the plane of

symmetry

```
8.77e-02
8.33e-02
7.89e-02
7.45e-02
7.01e-02
6.58e-02
6.14e-02
5.70e-02
5.26e-02
4.82e-02
4.38e-02
3.95e-02
3.51e-02
3.07e-02
2.63e-02
2.19e-02
1.75e-02
1.32e-02
8.77e-03
4.38e-03
0.00e+00
```
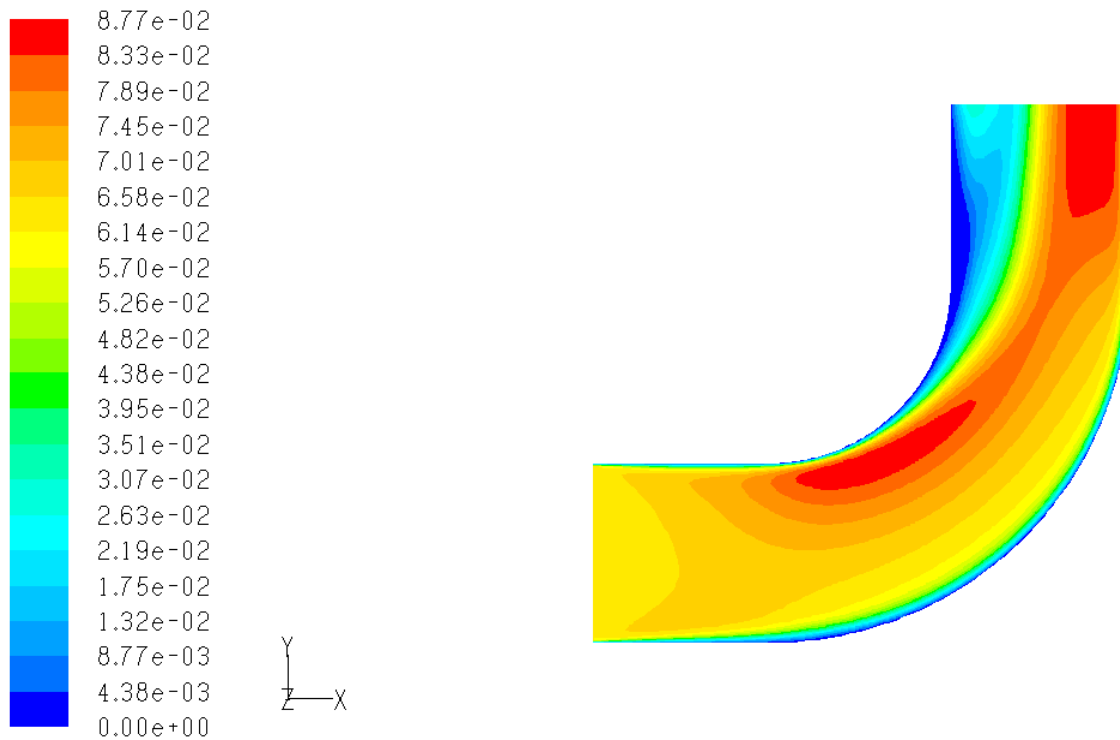
Figure 5.7 Contours of magnitude of velocity for n=0.6, N=1.0, Re=1100 in the plane of

symmetry

The above two contours, figures 5.6 and 5.7 are for shear thinning fluid, n=0.6 and for two Reynolds numbers, Re= 200, 1100. The value of the aspect ratio in both the cases is, N=1.0 as compared to that of a smaller aspect ratio in figures 5.1 and 5.2. Hence straight portion of the elbow in longer in the above two cases as compared that of the first two cases. For the case of lower Reynolds number, Re=200 the longer elbow has a circulation zone near the inner radius curvature but the shorter elbow does not have the recirculation zone.

As the length of the elbow further increases it can be seen that the amount of recirculation is higher in case of the lower Reynolds number than that for a higher Reynolds number. Figures 5.8 and 5.9 shows this phenomenon clearly. The two figures show the contours for n=0.75, Re=200, 1100 and N=5.0. From the results it can also be seen that the amount of recirculation is higher for a shear thinning fluid as compared to that of a shear thickening fluid for a longer elbow.
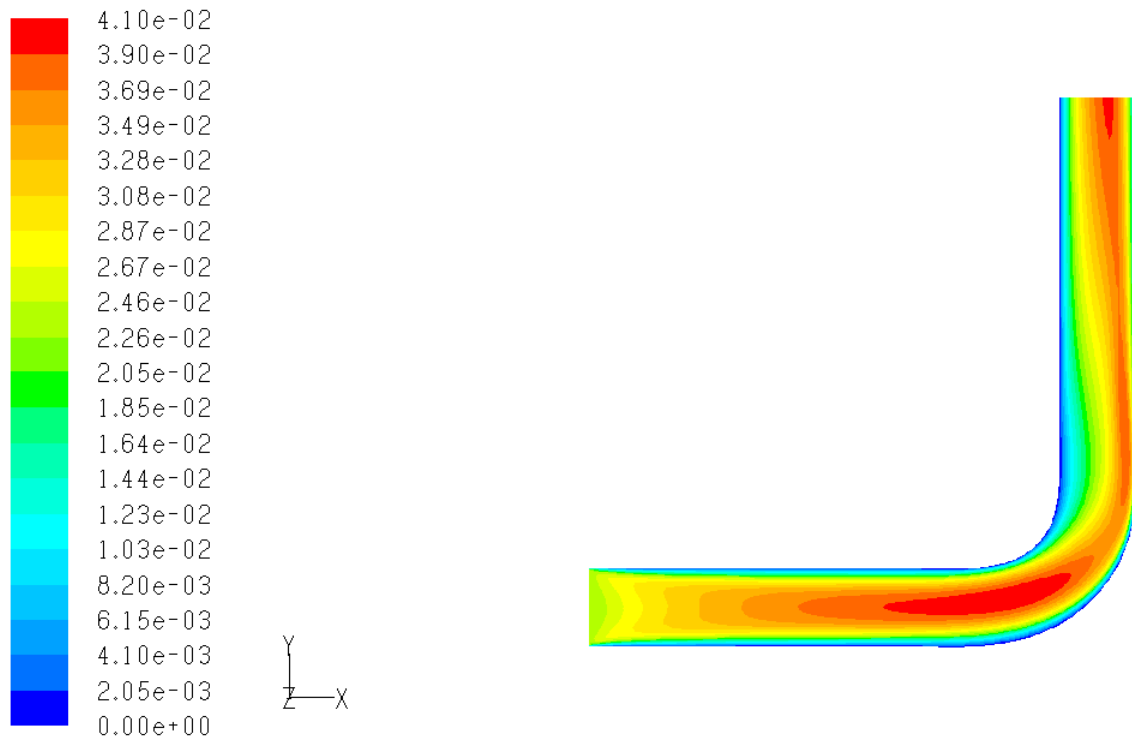

| 4.10e-02 |
| 3.90e-02 |
| 3.69e-02 |
| 3.49e-02 |
| 3.28e-02 |
| 3.08e-02 |
| 2.87e-02 |
| 2.67e-02 |
| 2.46e-02 |
| 2.26e-02 |
| 2.05e-02 |
| 1.85e-02 |
| 1.64e-02 |
| 1.44e-02 |
| 1.23e-02 |
| 1.03e-02 |
| 8.20e-03 |
| 6.15e-03 |
| 4.10e-03 |
| 2.05e-03 |
| 0.00e+00 |

Figure 5.8 Contours of magnitude of velocity for n=0.75, N=5.0, Re=200 in the plane of
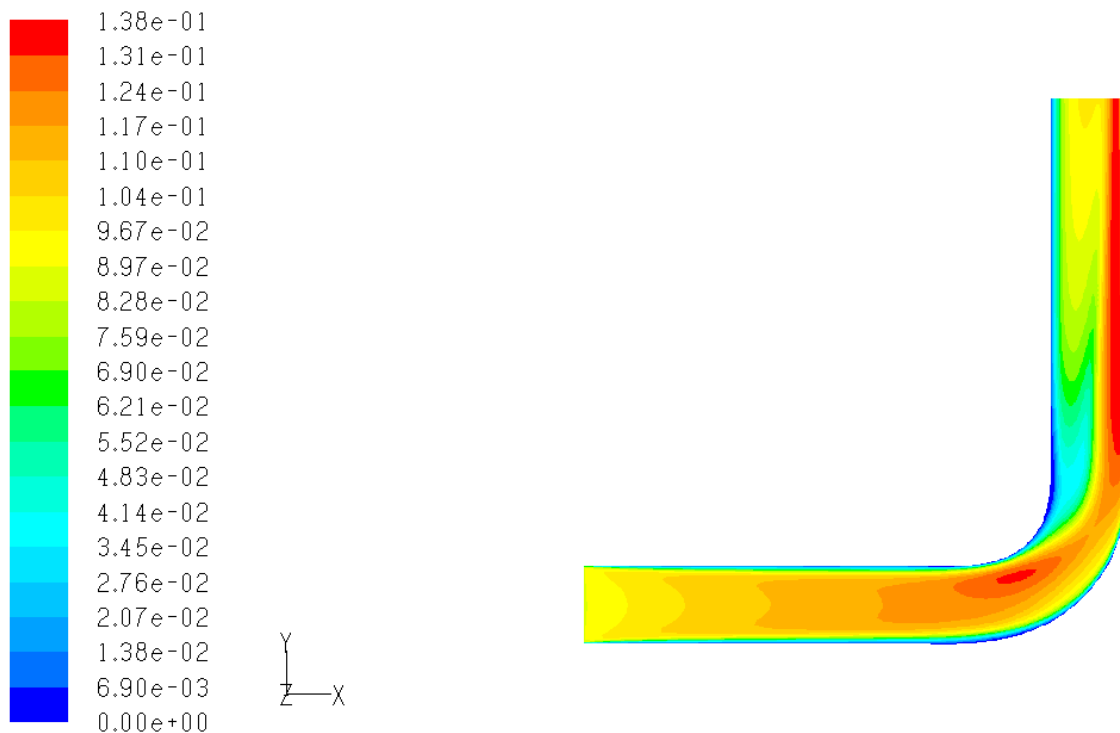
symmetry

Figure 5.9 Contours of magnitude of velocity for n=0.75, N=5.0, Re=1100 in the plane

of symmetry

Now, having studied the contours of velocity magnitude for different cases we go

into the details of the secondary flow in the elbow region. Figure 5.10 shows the nature

of the secondary flow in the elbow. Although the computations have been carried only in

the upper half of the domain since the problem is symmetric about the $Z = 0$ plane, the

results have been reflected about this plane the result has been shown for the whole

domain. The section shown below is the section formed at the midsection of the elbow

i.e., at an angle of $45°$ from the starting point of the curved section of the elbow. The

below view is the perspective view of the observer looking head-on with the inner radius

on the left and outer radius of the elbow on the right. The velocity vectors are properly scaled such that they can be clearly viewed in the elbow. The length and the direction of the velocity vector shows the magnitude of the velocity vector and the direction of the inplane velocity. The color of the velocity vectors indicates the magnitude of the velocity vectors and the scale on the window show the specified range. The below profile of velocity vectors is the case obtained for n= 0.75, N=1, Re=200.
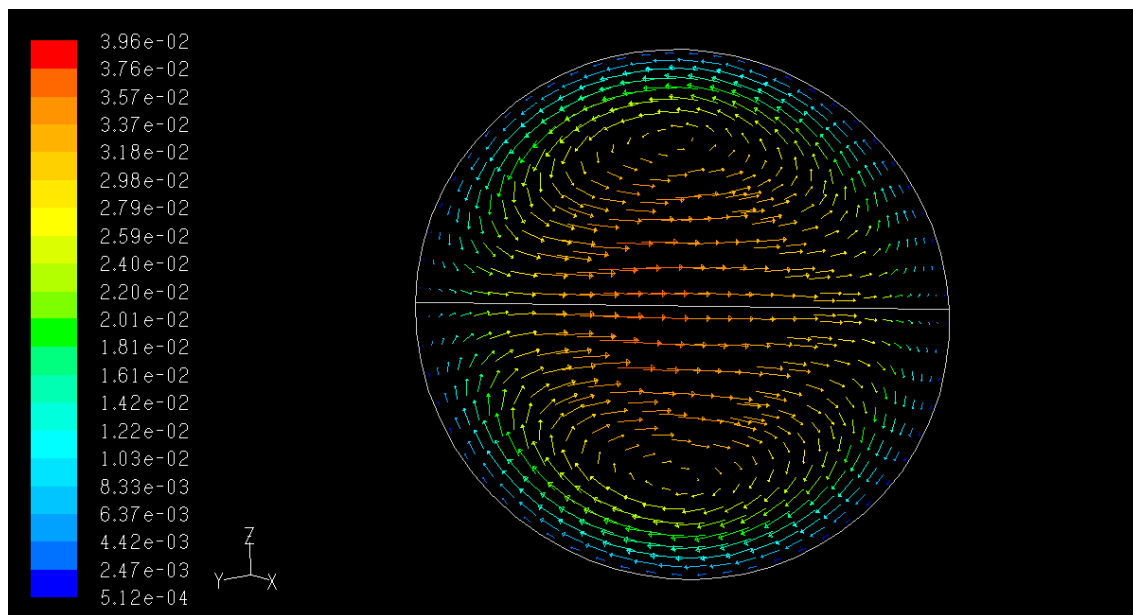

Figure 5.10 Two dimensional in-plane velocity vectors at the elbow midsection, $\theta = 45°$ with the color map indicating the three dimensional velocity magnitude

When the fluid enters the elbow section the fluid gets displaced from the center line to the outer radius due to the inertia effect. The fluid that reached the outer radius gets circulated back to the inner radius completing the loop. Thus the secondary flow consists of two vortices one in the upper half of the elbow and other in the lower half of the elbow. The loop in the upper half is in the counter-clockwise direction and that in the bottom half is in the clockwise direction. The axial velocity vectors of the particles along with the in-plane velocity vectors create a helical flow in the elbow.

Now we look into how the nature of the secondary flow varies with the variation of the Reynolds number. First consider the flow wherein the Reynolds number is low, Re=200. We can see that the center of the recirculation zone is more or less at the centre of the elbow. But, for higher Reynolds number the centre of the recirculation zone gets shifted towards the inner radius of the elbow for the same power law index and aspect ratio. Along with this it can also be seen that the magnitude of the secondary flow produced is higher in the case of higher Reynolds than that for a lower Reynolds number. Figures 5.11 and 5.12 shows the secondary flow at the midsection of the elbow for n=1.45, N=1 and Re=200, 1100 respectively. From here on only the top half of the cross section is shown and the results in the bottom half can be obtained by reflecting these results about the symmetry plane.
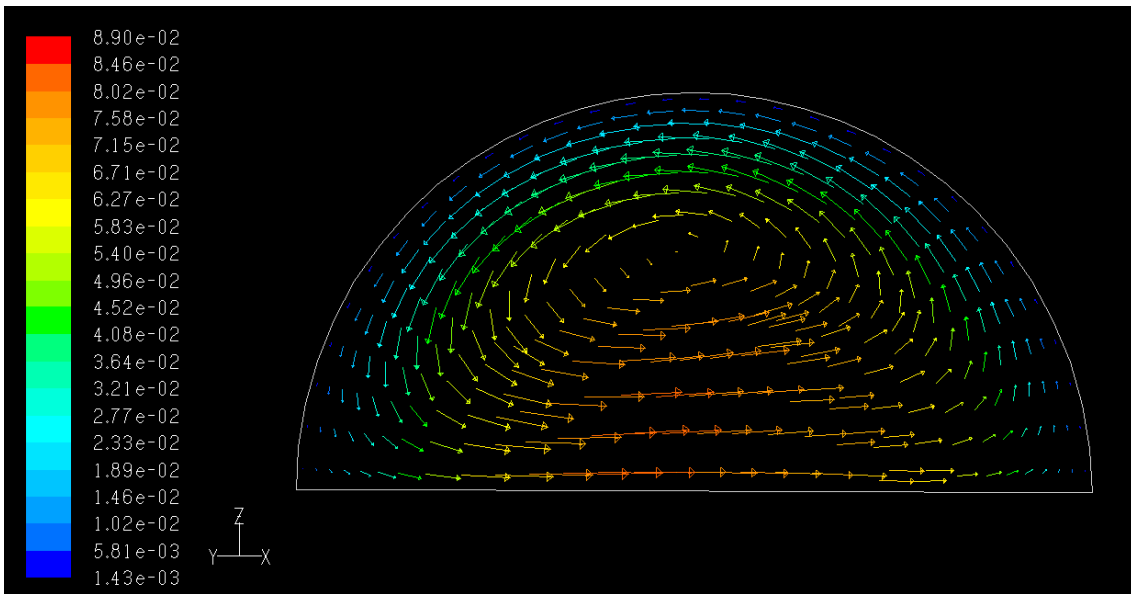
Figure 5.11 Two dimensional in-plane velocity vectors at the midsection representing

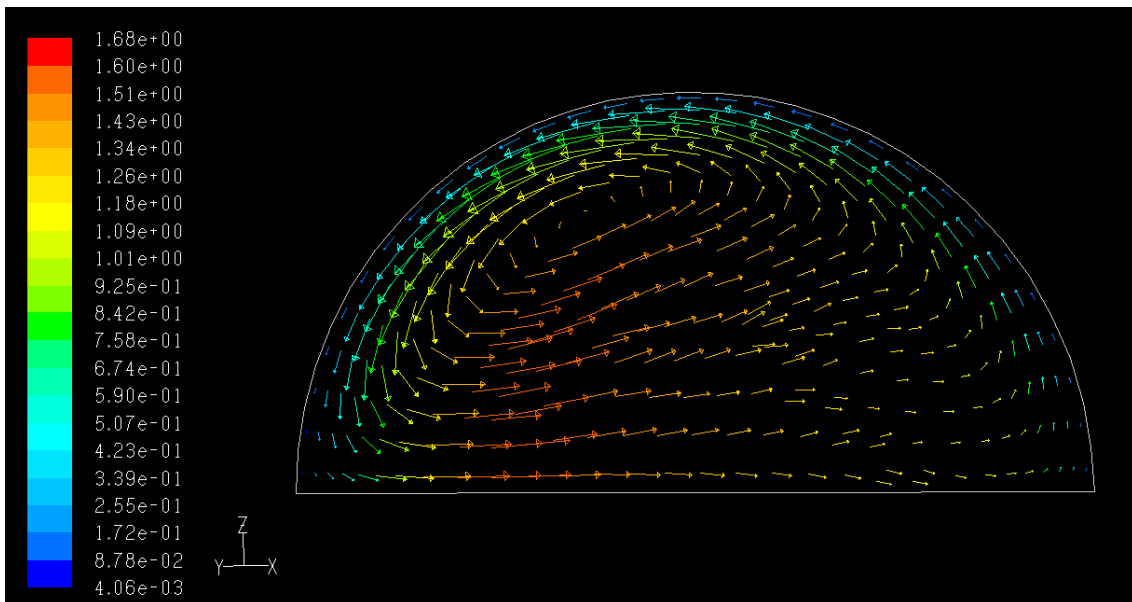the three dimensional velocity magnitude for n=1.45, N=1, Re=200
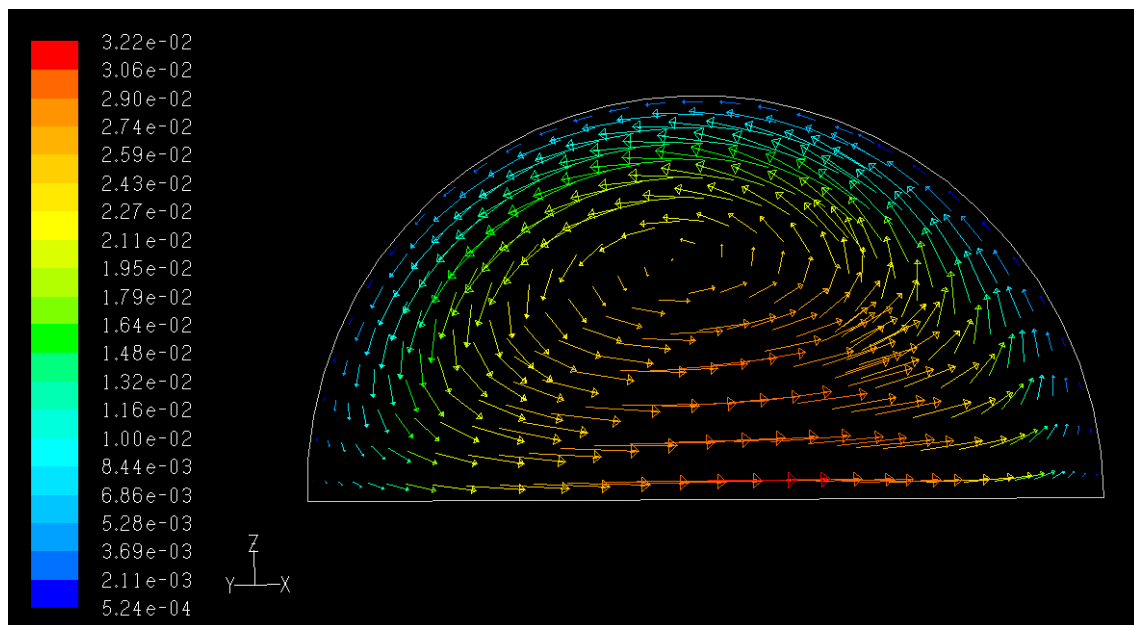

Figure 5.12 Two dimensional in-plane velocity vectors at the midsection representing

the three dimensional velocity magnitude for n=1.45, N=1, Re=1100

Now, we will look into the variation of the secondary flow with the variation of the power law index. We can note that the secondary flow for a shear thickening fluid is higher in magnitude than that for a shear thinning fluid. This can noted from the plots shown below (figures 5.13 and 5.14) for a power law index, n=0.6, 1.55 respectively. For this reason the dilatants fluids produce better heat transfer than the pseudoplastic fluids. Hence, dilatants fluids are better suited for heat exchangers due to their higher heat exchange rates. This is similar to the conclusion obtained by [9].

Figure 5.13 Two dimensional in-plane velocity vectors at the midsection representing

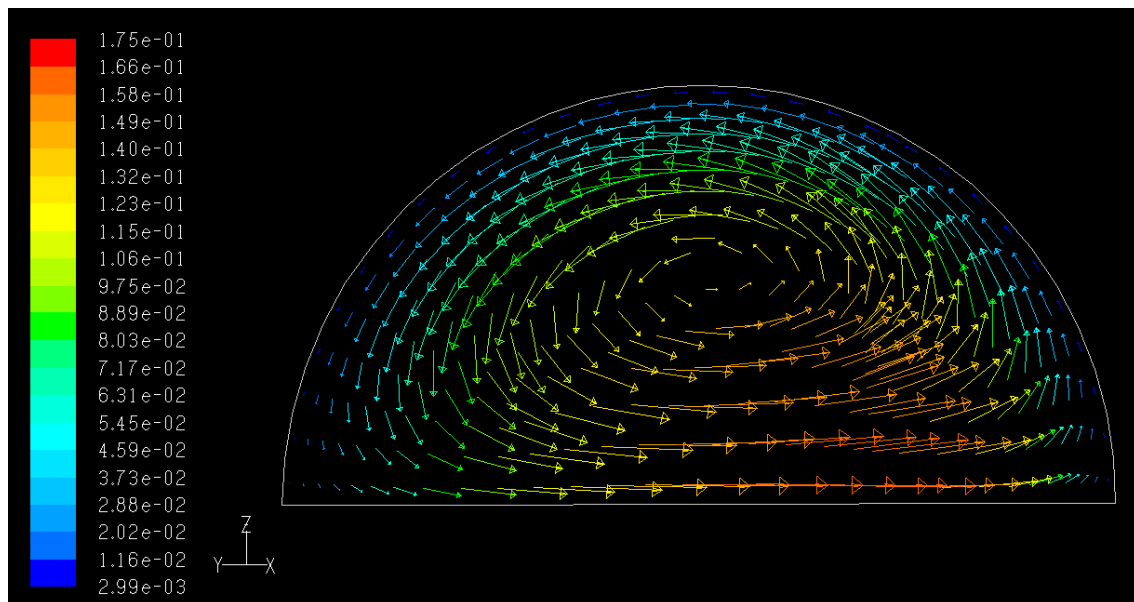the three dimensional velocity magnitude for n=0.6, N=5, Re=200

Figure 5.14 Two dimensional in-plane velocity vectors at the midsection representing

the three dimensional velocity magnitude for n=1.55, N=5, Re=200

The secondary flow does not vary much with the variation of the aspect ratio although there is some change in the velocity vectors with the largest aspect ratio having the highest magnitude of secondary flow.

Now we will look into the magnitude of the wall stress in the different regions of the elbow for different power law index, Reynolds number and aspect ratio. First, considering the general nature of the wall stress for a fluid flowing through an elbow, the magnitude of the stress is minimum at the outer radius in the first half of the elbow and at the inner radius in the second half of the elbow. It has the maximum value at the fluid inlet zone. Figure 5.15 below shows the wall stress profile for one of the cases n=0.75,

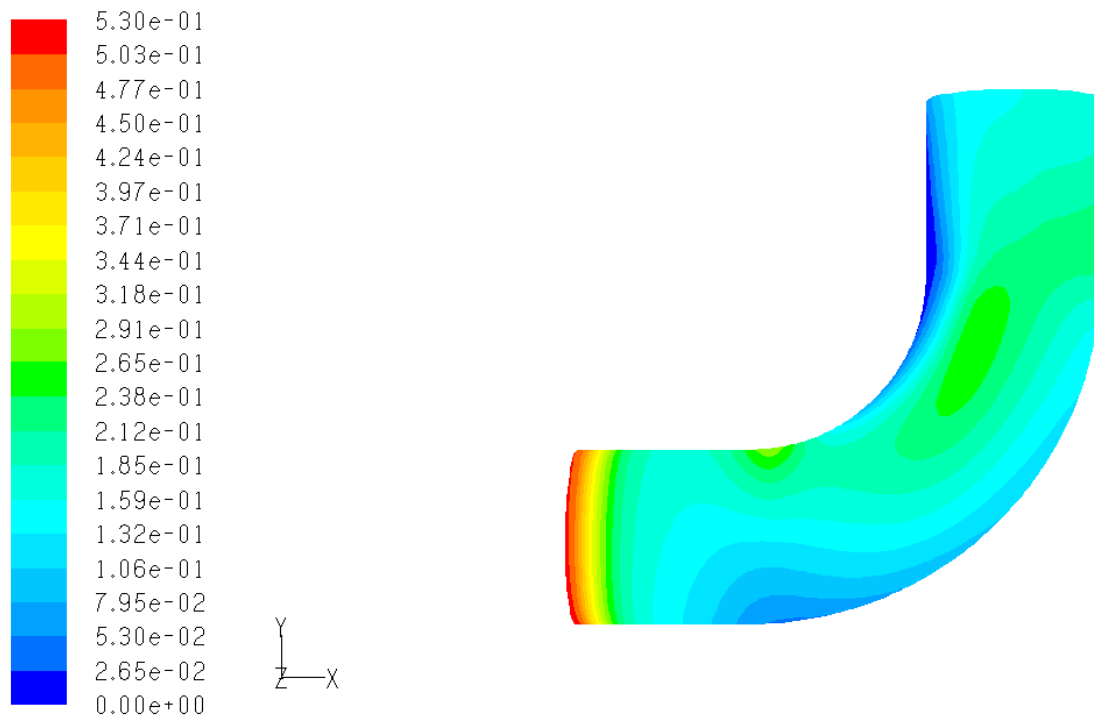N=1.0, Re=1100. The color scale indicates the magnitude of the wall stress in each region of the elbow.

Figure 5.15 Contours of wall stress on the elbow for n=0.75, N=1.0, Re=1100

Now, having seen the general nature of the wall stress in the elbow we will look into the variation of the wall stress with the power law index. The wall stress increases with the increase in the power law index of the fluid. So, shear thickening fluids in general have higher wall stress compared to the shear thinning fluid. Figures 5.16-5.18 shows the variation of the wall stress with the power law index.
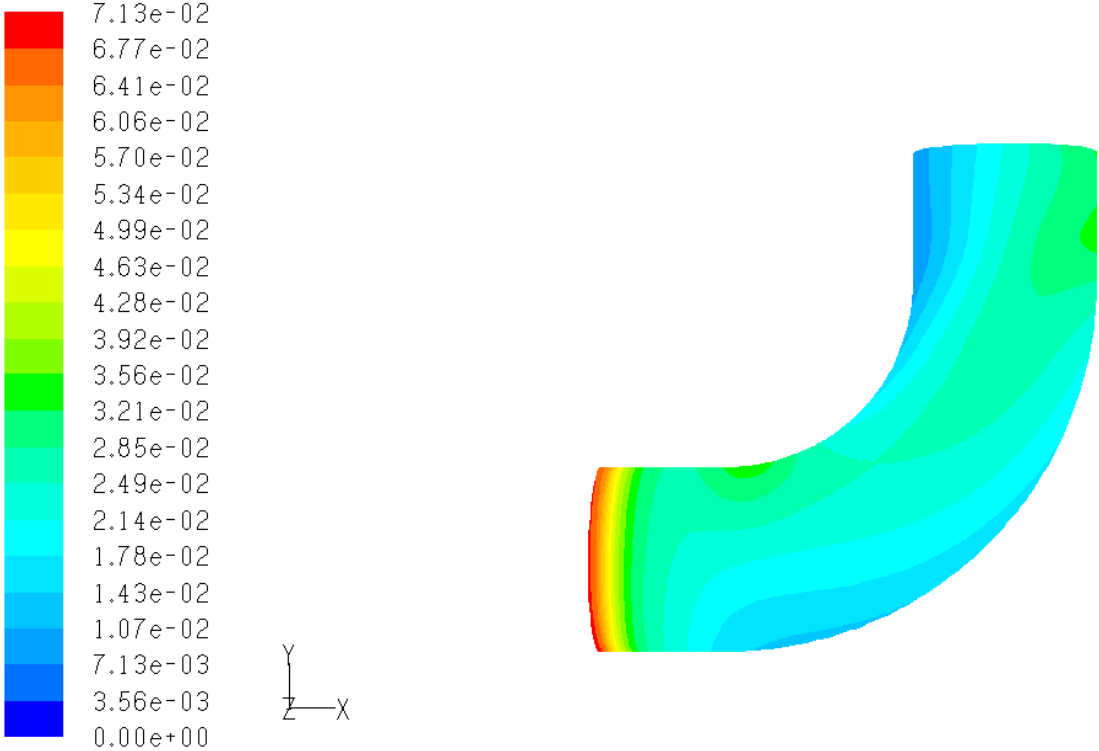
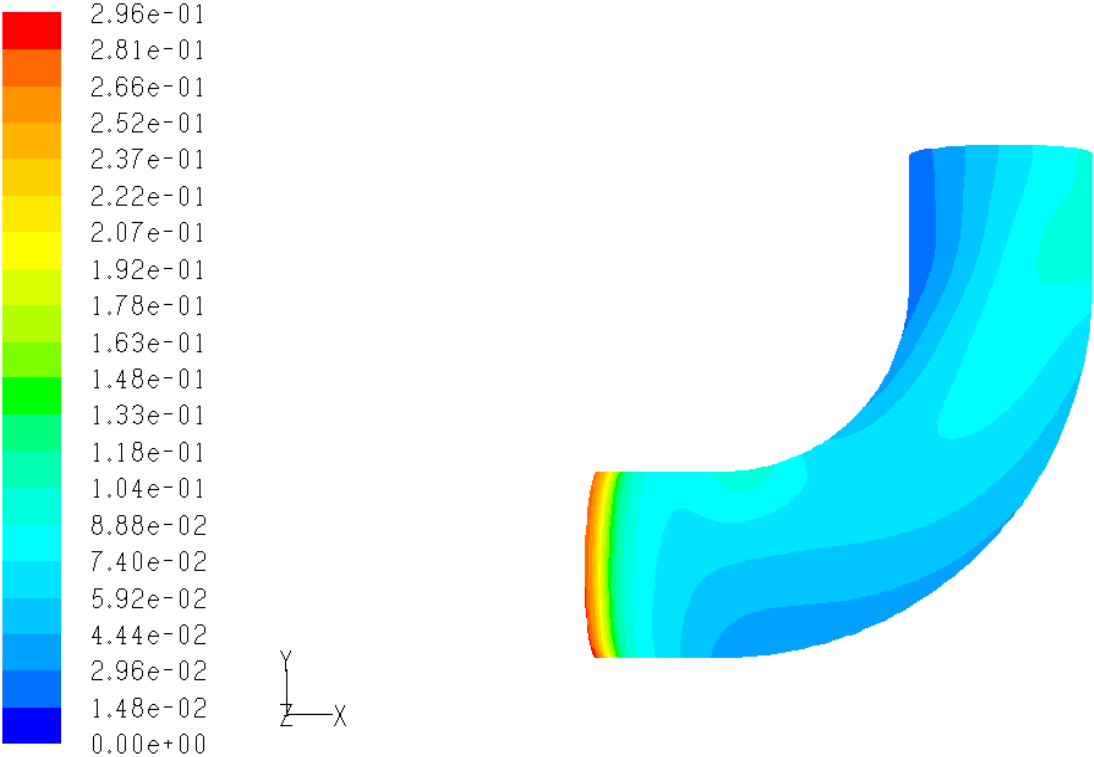Figure 5.16 Contours of wall stress on the elbow for n=0.60, N=0.7, Re=200

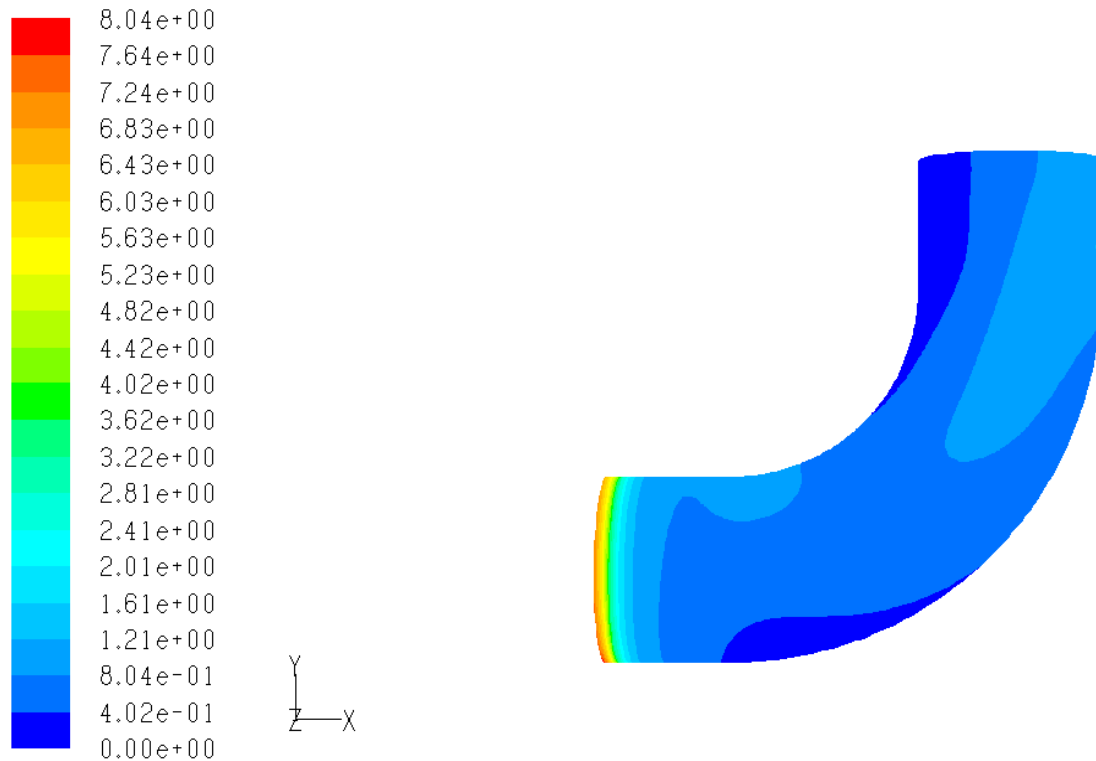Figure 5.17 Contours of wall stress on the elbow for n=0.90, N=0.7, Re=200

Figure 5.18 Contours of wall stress on the elbow for n=1.55, N=0.7, Re=200

It can also be seen from the figure 5.18 that the wall stress is relatively constant for a dilatants fluid and does not vary as much as that for a shear thinning fluid and the magnitude of shear stress is much higher for a shear thickening fluid. From the figures 5.19 and 5.20 it can be seen that the increase in the Reynolds number of the flow increases the magnitude of the shear stress on the elbow. With the increase in the Reynolds number of the flow the change of shear stress in different regions is substantial and is clearly visible.
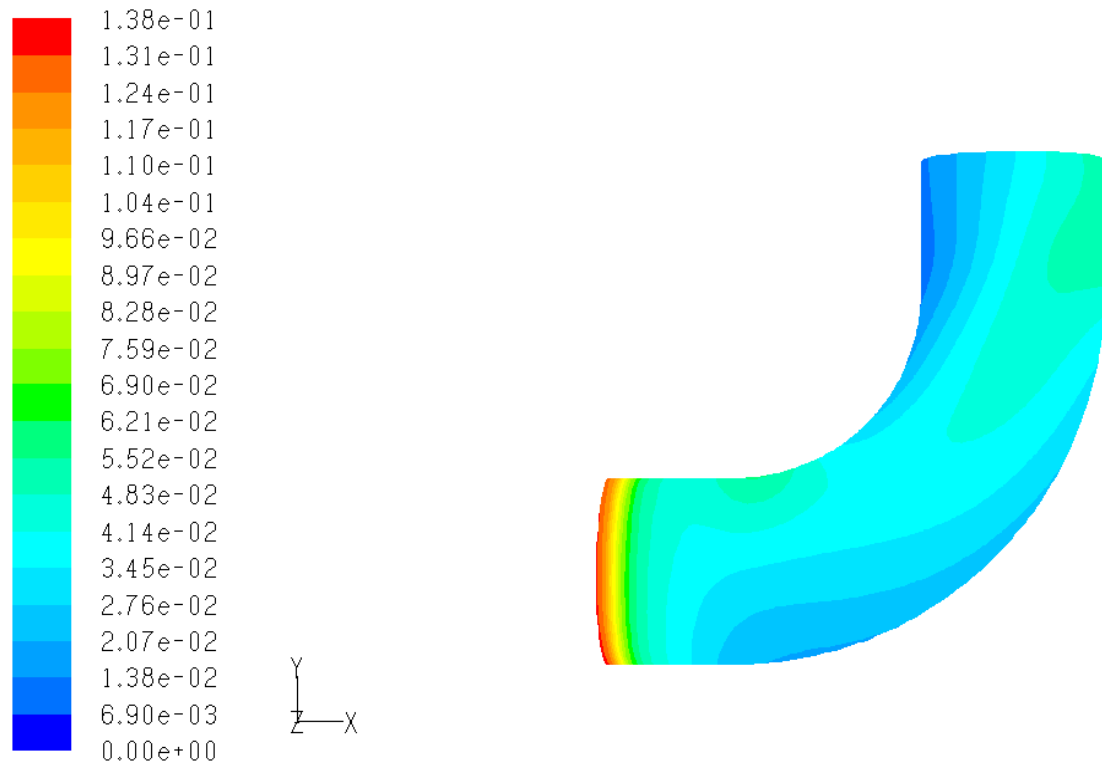
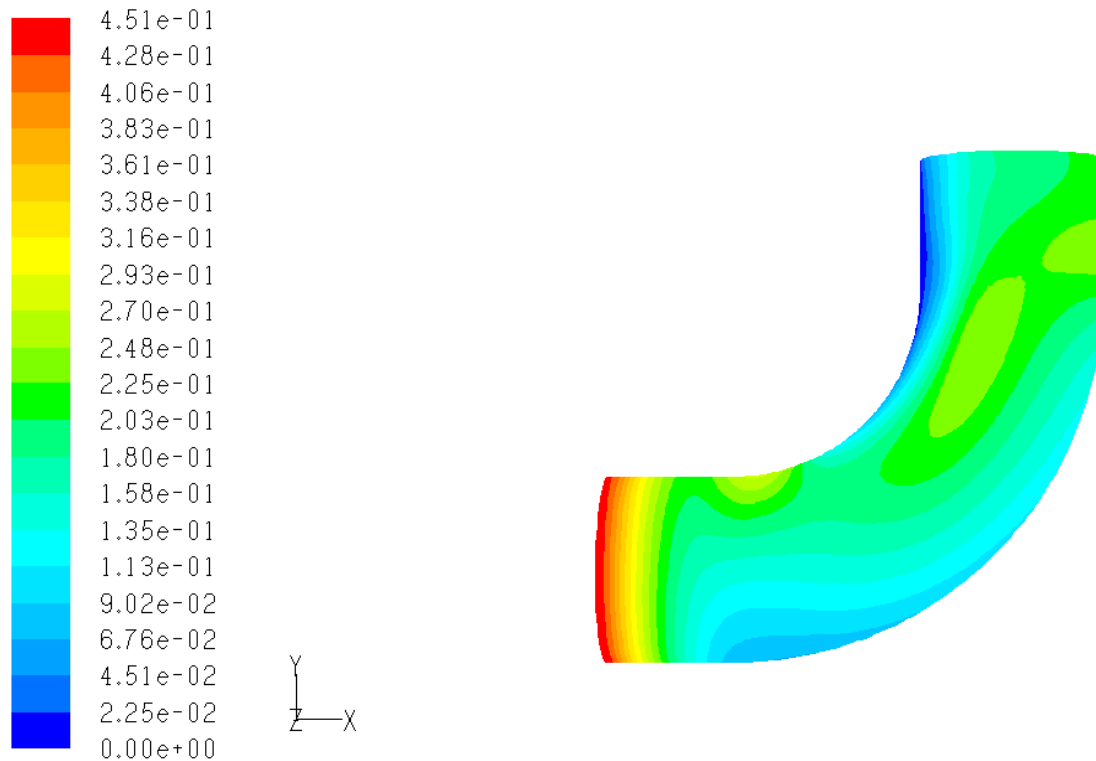Figure 5.19 Contours of wall stress on the elbow for n=0.75, N=0.7, Re=200

Figure 5.20 Contours of wall stress on the elbow for n=0.75, N=0.7, Re=1100

It is found that although the wall stress varies a little with the aspect ratio but the variation is not that significant and the variation for each of the aspect ratios is found to be similar.

In conclusion, the velocity profiles for the fluid flowing through have been obtained. These simulations have been done for a power law fluid considering both shear thickening and shear thinning cases. The flow considered in this analysis was assumed to be laminar. Also different elbow geometries have been considered to do the simulation in order identify the dependence of the velocity profiles on the shape of the elbow.

6. CHALLENGES FOR FUTURE WORK

The work done in this thesis mainly concentrated on obtaining the velocity profiles for the different cases considered and also performing the parametric analysis for the problem of flow of power law fluid in an elbow. Another important aspect that can be looked at in the future is to find out the dissipation from the fluid flowing through the elbow due to the change in the direction of flow. It is extremely important to study the amount of dissipation since it determines the amount of energy required to pump fluid through the elbow which is of practical importance in food and polymer processing industries. After determining the energy loss corresponding to each case the next step is to minimize these losses. So, one should optimize the bend so as to minimize the dissipation, given that the bend is within certain angle. The angle of the bend at which the dissipation is the least can be determined and bend can be designed at that particular angle so that the pumping power is minimized.

REFERENCES

[1] A. H. P. Skelland, *Non-Newtonian Flow and Heat Transfer*, New York: John Wiley, 1967.

[2] T. K. Bandyopadhyay and S. K. Das, "Non-Newtonian pseudoplastic liquid flow through small diameter components," *Journal of Petroleum Science and Engineering*, vol. 55, pp. 156-166, 2007.

[3] J. Marn and P. Ternik, "Laminar flow of a shear thickening fluid in a 90° pipe bend," *Fluid Dynamics Research*, vol. 38, pp. 295-312, 2006.

[4] T. K. Bandyopadhyay, T. K. Banerjee and S. K. Das, "Gas non-Newtonian liquid flow through elbows," *Chemical Engineering Communications*, vol. 182, no. 1, pp. 21-33, 2001.

[5] S. A. Berger, L. Talbot and L. S. Yao, "Flow in curved pipes," *Annual Reviews in Fluid Mechanics*, vol. 15, pp. 461-512, 1983.

[6] N. Arada, M. Pires and A. Sequeria, "Viscosity effects on flows of generalized Newtonian fluids through curved pipes," *Computers and Mathematics with Applications*, vol. 53, pp. 625-646, 2007.

[7] W. Y. Soh and S. A. Berger, "Fully developed flow in a curved pipe of arbitrary curvature ratio," *International Journal for Numerical Methods in Fluids*, vol. 7, pp. 733-755, 1987.

[8] S. C. R. Dennis, "Calculation of steady flow through a curved tube using a new finite difference method," *Journal of Fluid Mechanics*, vol. 99, no. 3, pp. 449-467, 1980.

[9] K. K. Raju and S. L. Rathna, "Heat transfer for flow of power law fluid in a curved tube," *Journal of Indian Institute of Science*, vol. 52, pp. 34-47, 1970.

[10] S. L. Rathna, "Flow of power law fluid in a curved pipe of circular cross-section," *Proceedings of Summer Seminar in Fluid Mechanics*, 1967, pp. 378-388.

[11] C. F. Hsu and S. V. Patankar, "Analysis of laminar non-Newtonian flow and heat transfer in curved tube," *AIChE Journal*, vol. 28, pp. 610-616, 1982.

[12] S. Agarwal, G. Jayaraman, V. K. Srivastava and K. D. P. Nigam, "Power law fluids in circular curved tube, Part-1 Laminar flow, Part-2 Axial laminar dispersion," *Polymer-Plastics Technology and Engineering*, vol. 32, pp. 587-635, 1993.

[13] T. Takami, K. Sudou and Y. Tomita, "Flow of non-Newtonian fluids in curved pipes," *Bulletin of JSME*, vol. 29, pp. 3750-3754, 1986.

[14] G. F. Homicz, "Computational fluid dynamic simulations of pipe elbow flow," *SAND Report*, SAND 2004-3467, 2004.

[15] J. Malek and K. R. Rajagopal, "Existence and regularity of solutions and the stability of rest state with shear dependent viscosity," *Mathematical Models and Methods in Applied Sciences*, vol. 5, no. 6, pp. 789-812, 1995.

[16] M. F. Edwards, M. S. M. Jadallah and R. Smith, "Head losses in pipe fittings at low Reynolds numbers," *Chemical Engineering Research and Design*, vol. 63, pp. 43-50, 1985.

[17] FLUENT Inc., *GAMBIT 2.3 User's Guide*, www.fluent.com, 2006.

[18] FLUENT Inc., *FLUENT 6.3 User's Guide*, www.fluent.com, 2006.

[19] S. V. Patankar, *Numerical Heat Transfer and Fluid Flow*, New York: McGraw-Hill, 1980.

VITA

Karthik Kanakamedala received his Bachelor of Technology degree in mechanical engineering from the National Institute of Technology Karnataka, India in 2007. He started his master's at Texas A&M University in August 2007 and received his Master of Science degree in December 2009.

Mr. Karthik Kanakamedala may be reached at Texas A&M University, Department of Mechanical Engineering, 3123 TAMU, College Station, TX 77843-3123, c/o Kumbakonam Rajagopal or by email at karthik.nitk@gmail.com.

The typist of this thesis was Karthik Kanakamedala.